



# On the mysterious Seychellois endemic spider genus *Cenemus* (Araneae, Pholcidae)

Bernhard A. Huber<sup>1</sup>, Guanliang Meng<sup>1</sup>

<sup>1</sup> Zoological Research Museum Alexander Koenig, LIB, Bonn, Germany

<https://zoobank.org/17BF9111-5551-410B-9703-0B0F3AAE867E>

Corresponding author: Bernhard A. Huber (b.huber@leibniz-lib.de)

Received 20 May 2022

Accepted 16 September 2022

Published 10 February 2023

Academic Editors Lorenzo Prendini, Anna Hundsdörfer

**Citation:** Huber BA, Meng G (2023) On the mysterious Seychellois endemic spider genus *Cenemus* (Araneae, Pholcidae). Arthropod Systematics & Phylogeny 81: 179–200. <https://doi.org/10.3897/asp.81.e86793>

## Abstract

The Pholcidae subfamily Smeringopinae has been revised extensively over the last decade, and most of its currently eight genera can now be placed with some confidence in the phylogeny of the family. A notable exception has been the endemic Seychellois genus *Cenemus* Saaristo, 2001. Morphologically, the genus is mainly characterized by plesiomorphies, which resulted in weakly supported and unstable positions in previous cladistic analyses. Molecular data have not previously been available. Here we revise the morphology of the type species *Cenemus culiculus* (Simon, 1898), including first SEM photos, and present the first molecular data for the genus. Morphology and molecules continue to give conflicting results regarding the sister taxon of *Cenemus*, but our analyses strongly support a position of the genus within the northern group of Smeringopinae (Northern Africa and the Mediterranean to India) rather than in the southern group (Subsahara Africa). This supports the idea that *Cenemus* is an ancient taxon, dating back to the breakup of Gondwana, between the separation of the Mascarene platform from Madagascar (~85 mya) and its separation from India (~60 mya). In addition, we present first molecular data for the recently established Smeringopinae genus *Maghreba* Huber, 2022, which is consistently resolved as sister to *Crossopriza* Simon, 1893; we present molecular evidence for the polyphyly of *Holocnemus* Simon, 1873, supporting previous morphological evidence; and we present an annotated list of the Pholcidae of the Seychelles, most of which are supposedly recent human introductions.

## Key words

Character conflict; Gondwana; island; morphology; molecules; relict; Smeringopinae

## 1. Introduction

Even though barely visible on a world map, the Seychelles are considered a micro-continent. This somewhat contradictory term emphasizes their uniqueness: the Granitic Seychelles are the only Far Islands that are not volcanic or coralline, and they are the only Far Islands that have been in contact with continental land masses (Stoddart 1984). This unique constellation probably explains why

the Seychelles have endemic amphibians, which in turn was a key criterion used by Wallace (1880) for his definition of continental versus oceanic islands (Nussbaum 1984). Some of the extant flora and fauna of the Seychelles is thought to be derived from ancient forms that existed on the Seychelles Bank before it separated from Africa, Madagascar, and finally from India about 60–70

mya (Collier et al. 2008). As would be expected from such an old history and long isolation, the Seychelles count numerous endemic genera, with varying affinities mainly to the Ethiopian and Oriental realms (Stoddart 1984; Procter 1984; Cogan 1984; Nussbaum 1984).

The existence of the endemic pholcid genus *Cenemus* Saaristo, 2001 on the Seychelles fits nicely into this picture. Pholcidae do not easily reach Far Islands. Except for introduced species, Pholcidae are absent from the Hawaiian Islands, from the South Atlantic Islands (Saint Helena, Ascension and Tristan da Cunha), from the Azores, and from New Zealand. Pholcid spiders have reached islands such as Galapagos, the Greater Antilles, the Canary Islands, and the Madeira Archipelago, but in all these cases the available data suggest a small number of independent introductions (and sometimes massive subsequent radiations) rather than multiple introductions (Dimitrov et al. 2008; Huber et al. 2010, 2022). To our knowledge, Pholcidae have never been observed to balloon, and natural introductions to islands must have happened via highly improbable means such as rafts or storms.

The phylogenetic affinities of *Cenemus* have proven difficult to resolve using morphology. As might be expected from a relict taxon, the genus is mainly characterized by plesiomorphic traits, which in turn means that there are very few synapomorphies linking it to other genera. At the level of subfamilies, at least, the affinities are clear: *Cenemus* is an uncontested member of Smeringopinae. This subfamily consists of two monophyletic groups: a northern group (Northern Africa and Mediterranean to Middle East and Central Asia), and a southern group (Subsahara Africa). Superficially, *Cenemus* is most similar to some representatives of *Smeringopus* Simon, 1890, a genus that is part of the geographically closer southern group. *Smeringopus* is species-rich in southern and eastern Africa, reaching Madagascar and the Comoros. Surprisingly, however, a first cladistic analysis of Smeringopinae (Huber 2012) tentatively placed *Cenemus* in the northern group. In a more recent morphological cladistic analysis (Huber 2022), *Cenemus* was excluded from the final analysis because its position was highly unstable in preliminary analyses (and because it did not seem to affect the focal genera of that analysis).

The present paper presents a detailed description of the morphology of *Cenemus*, with an emphasis on ultrastructure (which has not been studied before). We analyze this morphology in the light of a molecular phylogeny of Smeringopinae, newly adding *Cenemus* and a few other species to the extensive molecular phylogeny of Eberle et al. (2018).

## 2. Material and methods

### 2.1. Morphology

The morphological part of this study is based on the examination of 48 adult *Cenemus* specimens deposited

in Zoologisches Forschungsmuseum Alexander Koenig, Bonn, Germany (ZFMK) and Zoological Museum, Turku, Finland (ZMT). The taxonomic redescription follows the style of recent publications on Smeringopinae (e.g., Huber 2022; based on Huber 2000). Measurements were done on a dissecting microscope with an ocular grid and are in mm unless otherwise noted; eye measurements are  $\pm 5 \mu\text{m}$ . Photos were made with a Nikon Coolpix 995 digital camera (2048 $\times$ 1536 pixels) mounted on a Nikon SMZ 18 stereo microscope or a Leitz Dialux 20 compound microscope. CombineZP (<https://combinezp.software.informer.com>) was used for stacking photos. Drawings are based on photos that were traced on a light table and later improved under a dissecting microscope. Cleared epigyna were stained with chlorazol black. For SEM photos, specimens were dried in hexamethyldisilazane (HMDS) (Brown 1993), and photographed with a Zeiss Sigma 300 VP scanning electron microscope. The number of decimals in coordinates gives a rough indication about the accuracy of the locality data: four decimals means that the collecting site is within about 10 m of the indicated spot; three decimals: within  $\sim 100$  m; two decimals: within  $\sim 1$  km. The distribution map was generated with ArcMap 10.0.

### 2.2. Abbreviations

**ALE** – anterior lateral eye(s); **ALS** – anterior lateral spinneret(s); **AME** – anterior median eye(s); **a.s.l.** – above sea level; **L/d** – length/diameter; **PME** – posterior median eye(s); **PMS** – posterior median spinneret(s). Abbreviations used in figures only are explained in the figure legends.

### 2.3. Molecular phylogeny

#### 2.3.1. Taxon sampling

We used all Smeringopinae taxa from Eberle et al. (2018) and added the following: (1) 14 further species of Smeringopinae (newly sequenced), representing the genera *Cenemus*, *Crossopriza*, *Holocnemus*, and *Maghreba* (Table 1); (2) further *Holocnemus pluchei* (Scopoli, 1763) sequences taken from Bruvo-Mađarić et al. (2005), Dimitrov et al. (2012), and Wheeler et al. (2016); (3) 13 representatives of Pholcinae, the sister group of Smeringopinae, taken from Eberle et al. (2018); (4) a further outgroup taxon to root the tree (Arteminae: *Holocnemus huangdi* Tong & Li, 2009; taken from Eberle et al. 2018).

#### 2.3.2. Gene sampling

For the taxa taken from Eberle et al. (2018) we used all available sequences (CO1 barcode, 12S, 16S, 18S, 28S, and H3). For *Holocnemus pluchei* we used a total of four 12S, three CO1, two 18S, two 28S, and one H3 sequences (from the sources above). For *Cenemus culiculus* we

**Table 1.** Newly added taxa and their sequence accession codes. Detailed specimen information in Huber 2022 (*Crossopriza*, *Maghreba*, *Holocnemus*) and in main text (*Cenemus*); sorted alphabetically by genus and species.

Code	Genus	Species	Vial	Country	Administration	Locality	Lat	Long	COI	28S	H3
M089	<i>Cenemus</i>	<i>culiculus</i>	Sey24	Seychelles	Mahé	Bel Ombre	-4.6215	55.3957	ON504299	ON509570	ON497107
M081	<i>Crossopriza</i>	<i>dhofar</i>	Om130	Oman	Dhofar	Ain Razad cave	17.1301	54.2364	ON504292		
M083	<i>Crossopriza</i>	<i>dhofar</i>	Om144	Oman	Dhofar	E of Thumrait	17.6700	54.1630	ON504293		
M080	<i>Crossopriza</i>	<i>ghul</i>	Om105	Oman	Ad Dakhiliyah	Wadi Ghul	23.2340	57.1500	ON504291		
M084	<i>Crossopriza</i>	<i>kittan</i>	Om26	Oman	Ash Sharqiyah South	Wadi Tiwi	22.8010	59.2400	ON504294		
M085	<i>Crossopriza</i>	<i>moqal</i>	Om30	Oman	Ash Sharqiyah North	Moqal Cave	22.6240	59.0970	ON504295		
M086	<i>Crossopriza</i>	<i>salitan</i>	Om37	Oman	Al Batinah South	above Wadi Salitan	23.2200	57.3160	ON504296		
M088	<i>Holocnemus</i>	<i>hispanicus</i>	Rib34	Spain	Jaén	Cueva GEV-2	38.0310	-2.9920	ON504298		
M069	<i>Holocnemus</i>	<i>pluchei</i>	Mor105	Morocco	Béni Mellal-Khénifra	Imi n'Ifri	31.7240	-6.9720	ON504280		
M077	<i>Holocnemus</i>	<i>reini</i>	Mor94	Morocco	Drâa-Tafilalet	E Tamtetoucht	31.6860	-5.5210	ON504288		
M087	<i>Holocnemus</i>	<i>reini</i>	Rib33	Tunisia	Gafsa	near Bou Omrane	34.3500	9.1100	ON504297		
M079	<i>Maghreba</i>	<i>aurouxi</i>	Mor98	Morocco	Drâa-Tafilalet	SE Zebzat	32.6250	-4.5400	ON504290		
M071	<i>Maghreba</i>	<i>gharbija</i>	Mor111	Morocco	Marrakesh-Safi	4 km E Ghazoua	31.4490	-9.6880	ON504282		
M073	<i>Maghreba</i>	<i>gharbija</i>	Mor80	Morocco	Souss-Massa	Gourizim	29.6310	-10.0030	ON504284		
M076	<i>Maghreba</i>	<i>nkob</i>	Mor91	Morocco	Drâa-Tafilalet	E Nkob	30.8610	-5.8200	ON504287		
M078	<i>Maghreba</i>	<i>nkob</i>	Mor96	Morocco	Drâa-Tafilalet	N Errachidia	32.0396	-4.4214	ON504289		
M074	<i>Maghreba</i>	<i>saghro</i>	Mor86	Morocco	Souss-Massa	betw. Irherm & Tiferki	30.1406	-8.3337	ON504285		
M075	<i>Maghreba</i>	<i>saghro</i>	Mor89	Morocco	Souss-Massa	SE Tazenakht	30.5340	-7.0200	ON504286		
M070	<i>Maghreba</i>	<i>stifadma</i>	Mor106	Morocco	Marrakesh-Safi	near Toufliht	31.4715	-7.4332	ON504281		
M072	<i>Maghreba</i>	<i>stifadma</i>	Mor71	Morocco	Marrakesh-Safi	Setti-Fatma	31.2200	-7.6700	ON504283		

sequenced CO1, 28S, and H3; for all other newly added Smeringopinae taxa, we sequenced the CO1 barcode only. In total, there were 356 sequences and 105 specimens.

### 2.3.3. DNA extraction, amplification and sequencing

One or two legs of specimens stored in non-denatured pure ethanol (~99%) at -20° C were used for DNA extraction. Extracted genomic DNA is deposited at and available from the LIB Biobank, Museum Koenig, Bonn. DNA was extracted using the HotSHOT method (Truett et al. 2000). CO1 primers used were LCO1490-JJ and HCO2198-JJ (Astrin et al. 2016; primer versions JJ2 served as backup), but with a different tag sequence (from Srivathsan et al. 2021) of 13 bp length at the 5'-ends of forward and reverse primers, respectively. The 20 µl reaction volume consisted of 5 µl H<sub>2</sub>O, 1 µl DNA template, 2 µl Q-Solution, 10 µl Qiagen Multiplex-Mix, 1 µl forward primer, and 1 µl reverse primer. The PCR procedure was: (1) 95 °C for 15 minutes; (2) denaturation at 94 °C for 35 seconds; (3) annealing at 55 °C (or 40 °C) for 90 seconds; (4) elongation at 72 °C for 90 seconds; (5) final elongation at 72 °C for 10 minutes, followed by cooling at 10 °C. Steps 2–4 were repeated for 15 cycles (or 25 cycles). The PCR products were then pooled and sequenced with the Oxford Nanopore Technologies (ONT) GridON platform. All other parameters for PCR (incl. primers for 28S and H3) were as described in Eberle et al. (2018). PCR products were sent for bidirectional Sanger sequencing to BGI (Hong Kong, China).

### 2.3.4. DNA sequence alignment and editing

The H3 and 28S from Sanger-sequencing were assembled and aligned with Genious R7 (Kearse et al. 2012), and 20 CO1 sequences characterized by ONT sequencing were assembled using the ONTbarcode (Srivathsan et al. 2021) pipeline (ver. 0.1.8). Taxonomic assignments of the assembled sequences were checked by: (1) blasting assembled sequences against a local NT database; (2) the identification engine of the Barcode of Life Data System (BOLD) (<http://www.boldsystems.org/index.php>) (Ratnasingham and Hebert 2007; Yang et al. 2020).

### 2.3.5. Multiple sequence alignment (MSA)

For the protein-coding genes CO1 and H3, DNA sequences were translated into protein sequences using BioPython (version 1.78) (Cock et al. 2009) with invertebrate mitochondrial genetic code and standard genetic code, respectively. Next, protein-MSAs were constructed using the mafft-linsi algorithm of MAFFT (version 7.487) (Katoh and Standley 2013), which then assisted the construction of nucleotide level MSAs with pal2nal.pl (Suyama et al. 2006). This helps avoid the introduction of biologically meaningless frameshifts to the alignments (Suyama et al. 2006). The alignments of rRNA genes (12S, 16S, 18S, and 28S) were constructed based on secondary structure information using the mafft-xinsi algorithm in MAFFT (version 7.487) (Katoh and Standley 2013) and MXSCARNA (Tabei et al. 2008). Poorly aligned regions in the MSAs were then trimmed with Gblocks (version 0.91b) (Talavera and Castresana 2007) (-b5 = h), TrimAl (version 1.4.rev15) (Capella-Gutiérrez et al. 2009) (-automated 1) and ClipKIT (version 1.1.3) (Steenwyk et al. 2020), respectively. For the ClipKIT program, we tested different trimming strategies (--modes gappy, kpi, kpic, kpic-gappy, kpic-smart-gap, kpi-gappy, kpi-smart-gap, smart-gap).

### 2.3.6. Rogue taxa pruning

A second type of datasets was created by the exclusion of rogue taxa. Rogue taxa are taxa with different and contradictory positions in the tree set (Aberer et al. 2013), caused by ambiguous or insufficient phylogenetic signal (Sanderson and Shaffer 2002). Pruning rogue taxa from the analysis can improve resolution and/or node support values (Aberer et al. 2013). For each trimmed dataset, we ran multiple iterations of RogueNaRok (version 1.0) (Aberer et al. 2013) with a dropout size of 2 until no further rogue taxa were detected. Some taxa were not considered for pruning (-x option) due to their roles as target or rooting taxa in this study: *Cenemus culiculus* (M089) and the outgroup species *Holocneminus huangdi* (S348). The input data for RogueNaRok is a set of fully bifurcating unrooted bootstrap trees constructed by the following method: (1) MSAs of the six genes were firstly concatenated with the FASconCAT-G\_v1.05.pl program (Kück and Longo 2014), then gap-only sites were also trimmed out with TrimAl (version 1.4.rev15) (Capella-Gutiérrez et al. 2009); (2) next, 1000 rapid bootstrap trees were generated using RAxML (version 8.2.12) (Stamatakis 2014) and the GTRCAT model.

### 2.3.7. Phylogenetic inference

Maximum-likelihood trees were constructed based on concatenated alignments using IQ-TREE (version 2.1.3) (Minh et al. 2020) on the dataset with all specimens and the dataset with rogue taxa pruned, respectively. We applied an unpartitioned analysis (i.e., the whole concatenated MSA shares one evolutionary model) on each concatenated MSA. To overcome local optima during

heuristics, we performed 10 independent IQ-TREE runs (--runs 10) on each dataset, with a smaller perturbation strength (-pers 0.2) and larger number of stop iterations (-nstop 500). Branch supports were evaluated with 2000 ultrafast bootstrap (UFBoot) (Minh et al. 2013) with the risk of potential model violations considered (-B 2000 -bnni). SH-aLRT branch test (Guindon et al. 2010) was performed using 2000 bootstrap replicates (-alrt 2000). Best-fitting substitution models were automatically determined by the ModelFinder algorithm (Kalyaanamoorthy et al. 2017) in IQ-TREE. Tree visualizations were finished with the Newick utilities (version 1.6) (Junier and Zdobnov 2010) and iTOL (Letunic and Bork 2021). We also tested the coalescence-based tree construction strategy using IQ-TREE (version 2.1.3) (Minh et al. 2020) and ASTRAL (version 5.7.8) (Zhang et al. 2018). However, these analyses resulted in many polytomies and often failed to recover uncontested clades, presumably due to missing data. Therefore, we did not further consider these trees.

## 3. Results

### 3.1. Molecular phylogeny

The tree in Fig. 1 shows the northern group of Smeringopinae resulting from one of the analyses using all taxa (i.e., including rogue taxa). The tree was chosen due to its high support values for the uncontested clades Pholcinae and Smeringopinae. The entire tree (including the southern group and showing support for each node in other analyses) is shown in Supplementary Figure S1. A tree excluding rogue taxa is shown in Supplementary Figure S2.

Our analyses were highly consistent in recovering the northern and southern groups of Smeringopinae, usually with high support values for each of them. All analyses placed *Cenemus* in the northern group of Smeringopinae, as sister to a group that included all representatives of the “spotted leg clade” sensu Huber (2022), except *Holocneminus pluchei* and *Hoplopholcus*.

Apart from *Cenemus*, our analyses provide strong support for (1) a sister group relationship between *Crosso-priza* and *Maghreba*; and (2) a sister group relationship between the preceding clade and *Holocneminus reini* (C. Koch, 1873) [and its sister taxon *Holocneminus caudatus* (Dufour, 1820)]. Our analyses thus provide further support for the non-monophyly of *Holocneminus*. However, the proposed sister group relationships between (1) *Holocneminus pluchei* and *Hoplopholcus* Kulczyński, 1908, and (2) between *Holocneminus hispanicus* Wiehle, 1933 and *Stygopholcus* Kratochvil, 1932, received either low support or were not recovered at all.

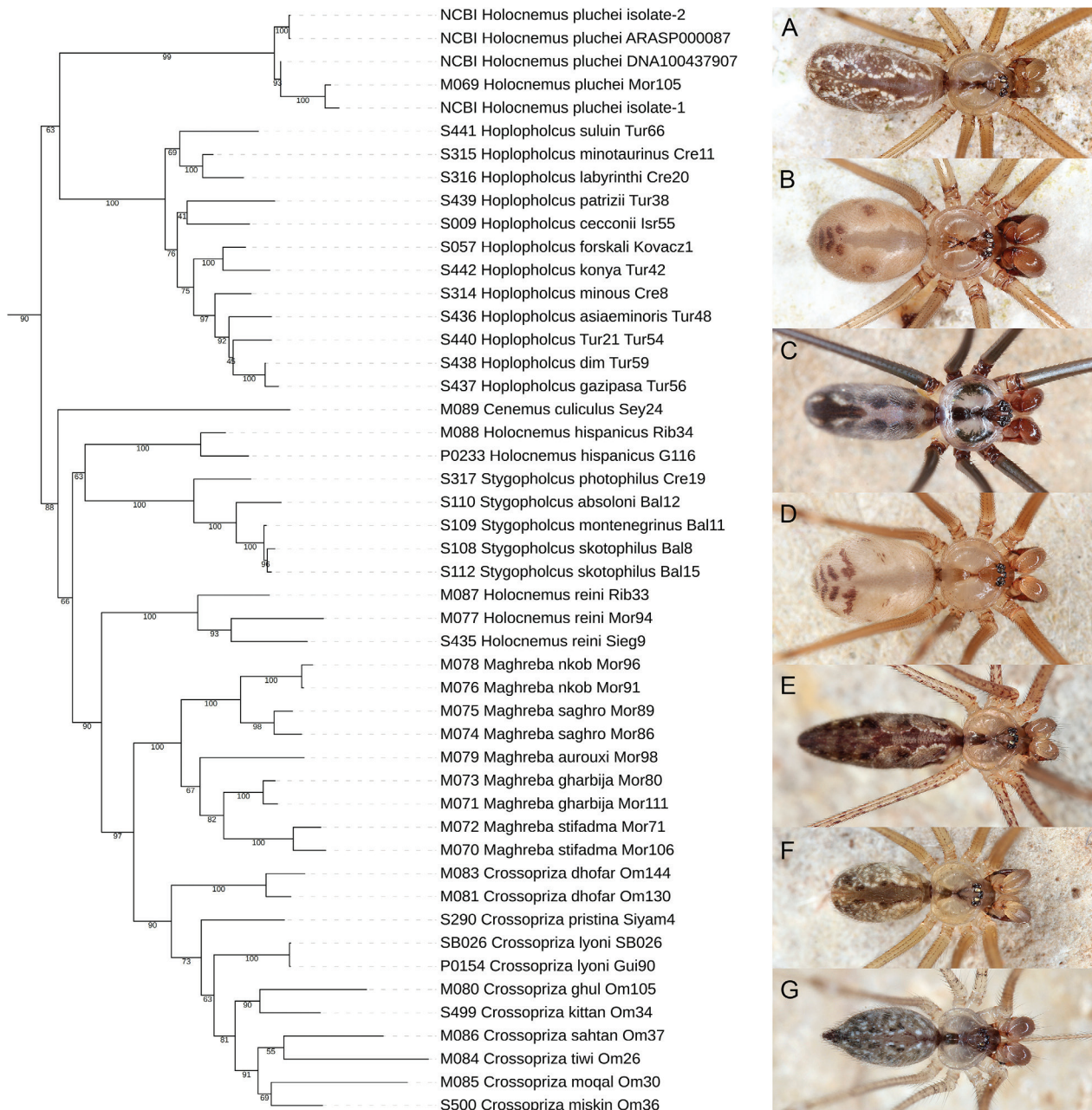


**Figure 1.** Molecular phylogeny of the northern group of Smeringopinae as resolved by IQ-TREE, gene alignments trimmed with ClipKit's smart-gap strategy, and rogue taxa included. Branch support values are ultrafast bootstrap (UFBoot) supports (%). Terminals are composed of specimen code, species name, and ZFMK collection vial code. For complete tree and for support of individual nodes in other analyses, see Supplementary Figure S1. Photos: **A** *Holocnemus pluchei*. **B** *Hoplopholcus patrizii*. **C** *Cenemus culiculus*. **D** *Stygopholcus skotophilus*. **E** *Holocnemus reini*. **F** *Maghreba stifadma*. **G** *Crossopriza dhofar*.

## 3.2. Taxonomy

### 3.2.1. Genus *Cenemus* Saaristo, 2001 (Family Pholcidae C.L. Koch, 1850)

*Cenemus* Saaristo, 2001: 19 (type species: *Holocnemus culiculus* Simon, 1898).

**Description.** The three species currently included in this genus are extremely similar to each other. The redescription of the type species below thus covers the genus except for some minor details of the genitalia (cf. Saaristo 2001, 2002).

**Diagnosis.** Large, long-legged pholcids with deep carapace pit and cylindrical abdomen; distinguished from similar Smeringopinae (especially *Smeringopus*; also *Holocnemus* and *Smeringopina* Kraus, 1957) by the combination of: (1) male gonopore with six epiandrous spigots (Fig. 31; only two in *Smeringopus* and *Smeringopina*); (2) ALS with only two spigots each (Fig. 63; seven to eight in *Smeringopus* and *Smeringopina*); (3) male chelicerae with one pair of apophyses, each with one conical hair at tip (Fig. 33; two or more hairs in certain *Holocnemus* and other Smeringopinae; some Smeringopinae without conical hairs); (4) male and female chelicerae with distinct stridulatory files (Figs

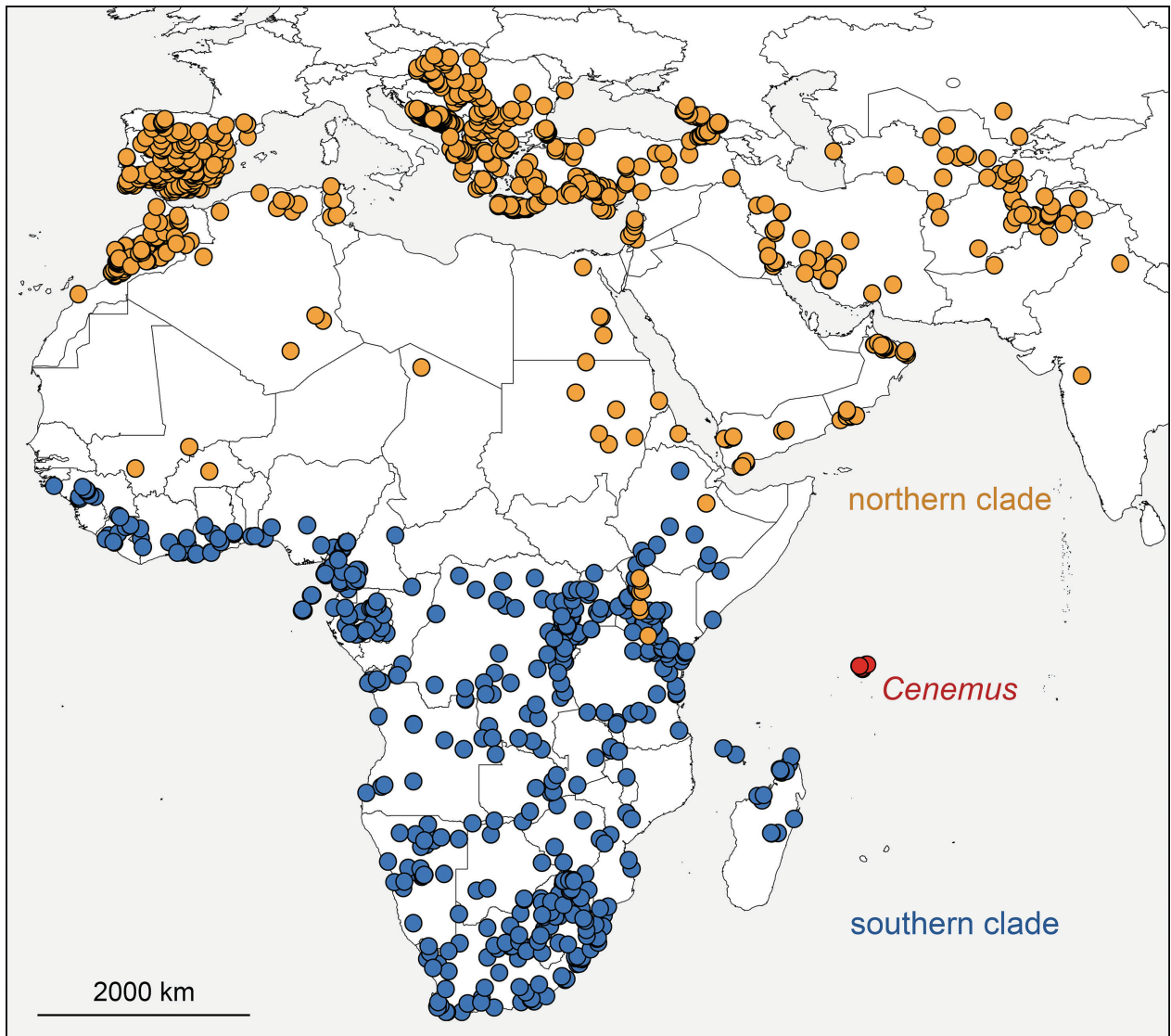


**Figure 2.** Known distributions of the northern and southern groups of Smeringopinae and of *Cenemus*. Excluded from this map are three widely distributed synanthropic species: *Holocnemus pluchei* (Scopoli, 1763); *Crossopriza lyoni* (Blackwall, 1867); and *Smeringopus pallidus* (Blackwall, 1858). Also excluded are Australian records of *Smeringopus natalensis* Lawrence, 1947. Note that the southern group ranges into the southern Arabian Peninsula but the respective blue dots are covered by orange dots.



**Figures 3–4.** Typical habitat of *Cenemus culiculus* (Simon, 1898) on Mahé, Casse Dent (arrow points at preferred microhabitat of adults), and web of *C. culiculus* (Mahé, Bel Ombre).

36, 49; absent in *Smeringopus* and *Smeringopina*); (5) palpal tarsus without macrotrichia (Figs 9–11; often present in *Smeringopus* and *Smeringopina*); (6) procurus tip without ventral spine (Fig. 20; present in most other Smeringopinae); (7) male anterior femora without spines (present in *Holocnemus*, *Crossopriza*, *Stygopholcus*, and *Hoplopholcus*); (8) prolateral trichobothrium of tibia 1 absent (present in *Smeringopus* and *Smeringopina*); (9) tarsal pseudosegments distinct (Fig. 56; indistinct in all other Smeringopinae); (10) leg tarsal organs oval, with indentation in proximal median part of rim (Figs 58–61; round and without indentation in all other Smeringopinae).

**Natural history.** Nothing has been published about the biology of *Cenemus* before. Given the high general similarity of the three known species, the basic observations on *C. culiculus* below are probably valid for all of them.

**Relationships.** *Cenemus* is part of the northern group of Smeringopinae. Its sister group remains unclear (see Discussion).

**Composition and distribution.** Three species endemic to the Seychelles (Fig. 2): *Cenemus culiculus* (Simon, 1898) (Mahé and Silhouette); *C. silhouette* Saaristo, 2001 (Silhouette); and *C. mikehilli* Saaristo, 2002 (La Digue and Marianne). All available evidence suggests that *Cenemus* is indeed restricted to the Granitic Seychelles. Given the size of the spider and the easily visible large webs, it seems very unlikely that *Cenemus* has been overlooked in other regions.

### 3.2.2. *Cenemus culiculus* (Simon, 1898)

Figs 5–63

*Holocnemus culiculus* Simon, 1898: 375 (juv.); Saaristo 1978: 103, figs 27–30, 39–45 (♂♀).

*Cenemus culiculus* (Simon, 1898); Saaristo 2001: 19, figs 36–41, 47–48; Saaristo 2010: 160, figs 25.6–15 (text and figures copied from previous papers, with errors, e.g. regarding material of *C. mikehilli* listed under *C. culiculus*).

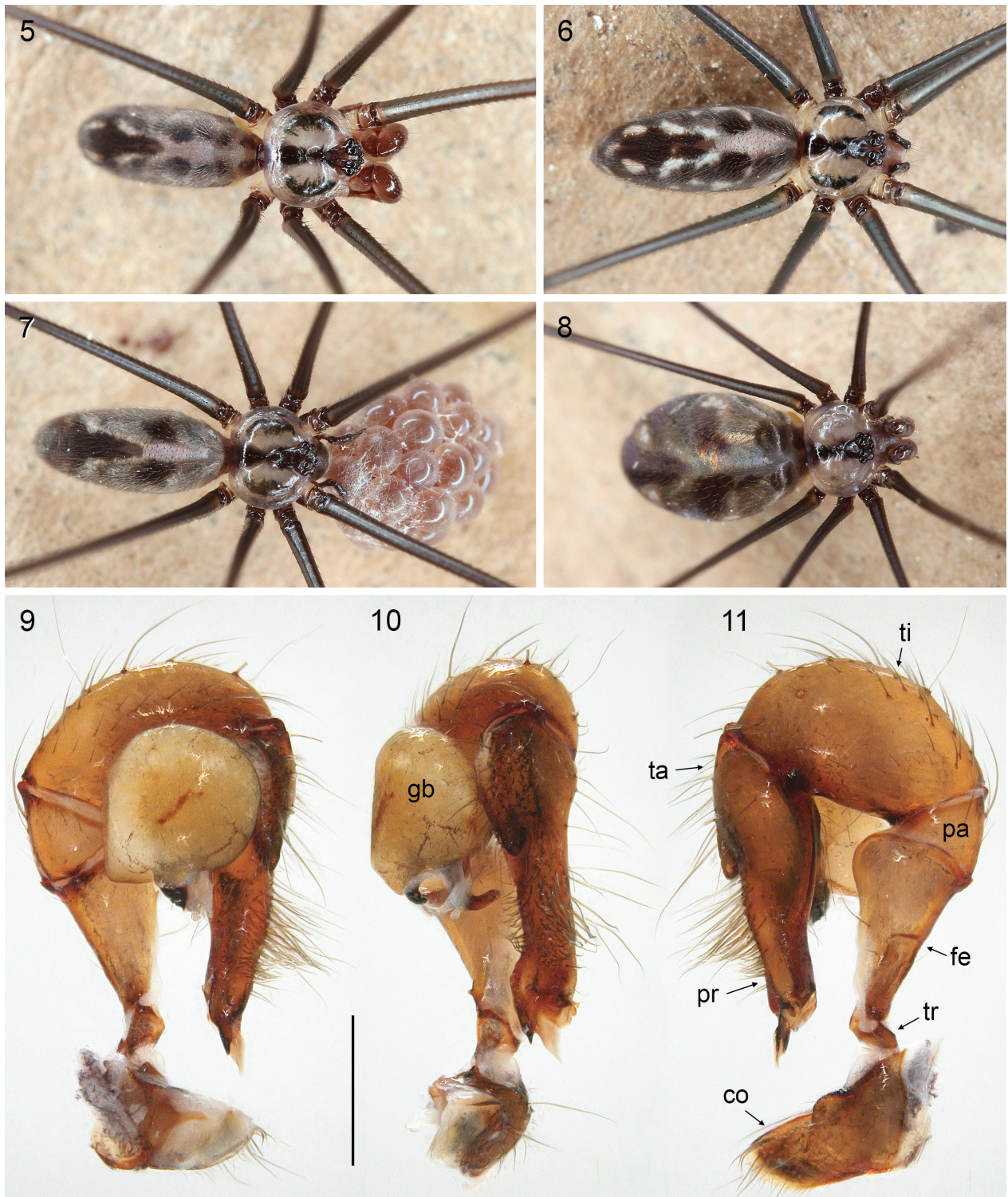
**Diagnosis.** See Saaristo (2001, 2002) for morphological differences between the three nominal species. Interspecific relationships are beyond the scope of this study.

**Type.** SEYCHELLES – Mahé • 1 juvenile holotype, examined; precise locality not identified; 1895; A. Brauer leg.; MNHN 10343, with E. Simon's handwritten label "15220 *Hol. culicinus* [sic!] ES, Ins. Sechelles (Brauer)".

**Material examined.** SEYCHELLES – Mahé • 1 ♂, 2 ♀♀; Anse Boileau, Glacis La Reserve; 4.7070°S, 55.5007°E; 230 m a.s.l.; 7 Mar. 2013; C. Hoareau leg.; ZFMK Ar 23864 • 1 ♂ in pure ethanol; same data as preceding; ZFMK Sey25 • 1 ♂, 2 ♀♀; Bel Ombre, "site 2"; 4.6215°S, 55.3914°E; 80 m a.s.l.; 6 Mar. 2013; C. Hoareau leg.; ZFMK Ar 23865

• 1 ♀ in pure ethanol; same data as preceding; ZFMK Sey28 • 7 ♂♂, 6 ♀♀; Bel Ombre, "site 1"; 4.6215°S, 55.3957°E; 70 m a.s.l.; 6 Mar. 2013; C. Hoareau leg.; ZFMK Ar 23866 • 2 ♀♀, 1 juv., in pure ethanol; same data as preceding; ZFMK Sey24 • 1 ♂, 3 ♀♀; Port Glaud, Casse Dent; 4.648°S, 55.428°E; 450 m a.s.l.; 8 Mar. 2013; C. Hoareau leg.; ZFMK Ar 23867 • 1 ♀ in pure ethanol; same data as preceding; ZFMK Sey27 • 7 ♂♂, 8 ♀♀; Port Glaud, Morne Blanc; 4.6559°S, 55.4388°E; 430 m a.s.l.; 4 Mar. 2013; C. Hoareau leg.; ZFMK Ar 23868 to 23869 • 2 ♀♀, 4 juvs, in pure ethanol; same data as preceding; ZFMK Sey22 • 1 ♀; Port Glaud, near Cap Ternay; 4.6452°S, 55.3883°E; 40 m a.s.l.; 4 Mar. 2013; C. Hoareau leg.; ZFMK Ar 23870. — **Silhouette** • 1 ♂, 1 ♀, see Remarks below; Jardin Marron; 4.48°S, 55.24°E; 20 Jan. 1999; M. Saaristo and J. Gerlach leg.; MZT (without number; presumably taken from MZT AA 1108 to 1110).

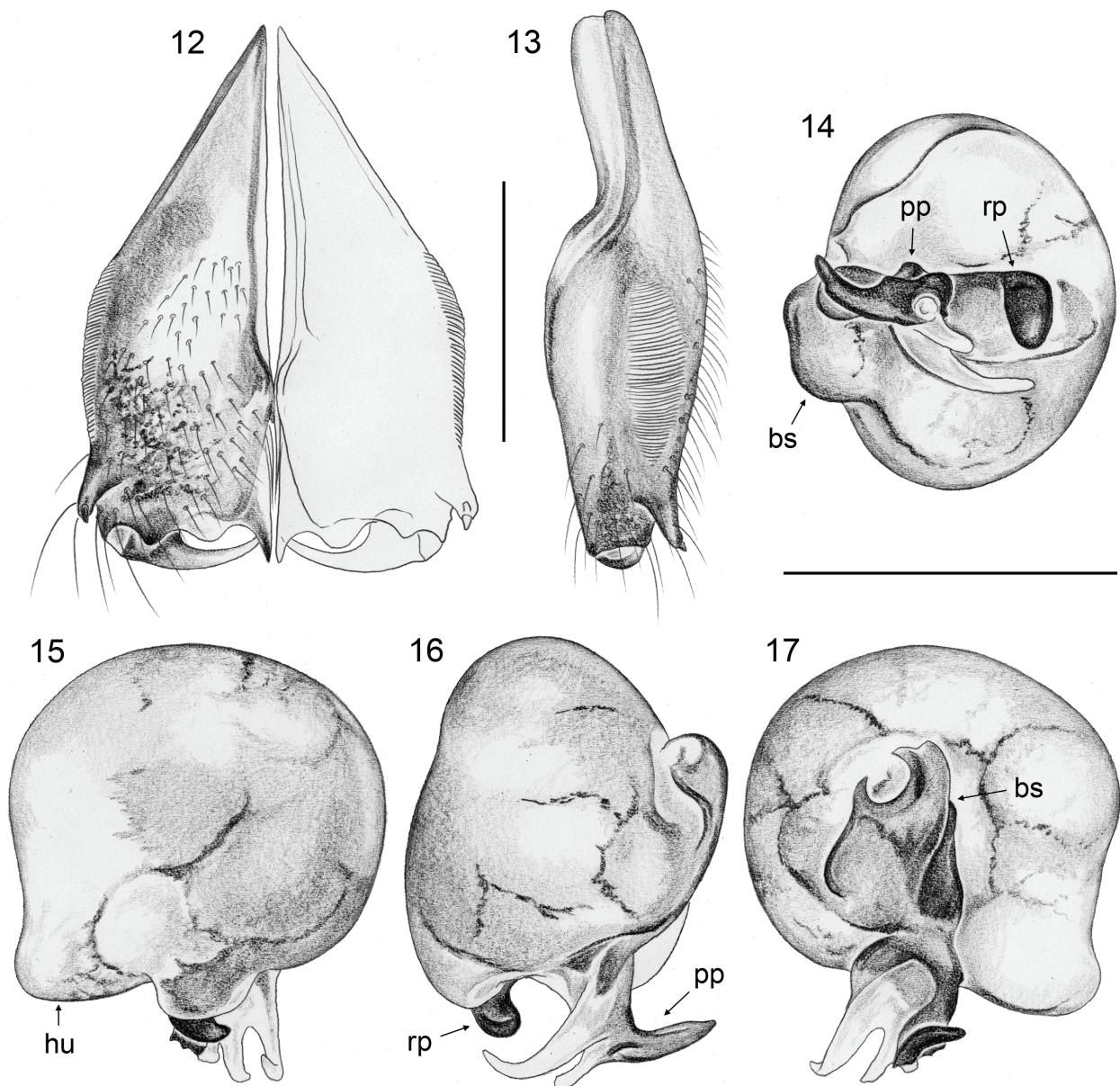
**Redescription. Male** (ZFMK Ar 23866) — MEASUREMENTS. Total length 6.5, carapace width 2.2. Distance PME–PME 100 µm; diameter PME 160 µm; distance PME–ALE 100 µm; diameter AME 110 µm; distance AME–AME 30 µm. Leg 1: 59.4 (14.7 + 0.9 + 14.5 + 25.7 + 3.6), tibia 2: 8.7, tibia 3: 6.2, tibia 4: 7.3; tibia 1 L/d: 55; femora 1–4 diameters at half length: 0.40, 0.31, 0.30, 0.30. — COLOR (in ethanol). Carapace pale ochre with median brown band including ocular area and pair of submarginal lateral bands (Fig. 5); clypeus light brown; sternum dark brown, with lighter brown median mark, narrow lateral light bands, and dark brown lateral margins; legs brown, femora and tibiae with light tips and dark brown to black subdistal rings; abdomen ochre–gray, with dark marks dorsally and laterally, ventrally with large black marks in front of gonopore and at spinnerets, with lighter brown diffuse median band behind gonopore. — BODY. Habitus as in Fig. 5. Ocular area raised; each secondary eye with small accompanying elevation (Fig. 30). Carapace with short but deep thoracic pit dividing posteriorly into pair of diverging shallow furrows extending toward posterior margin (Fig. 29). Clypeus unmodified, only rim slightly more sclerotized than in female and median stripe with slightly different cuticle (as in female; cf. Fig. 48). Sternum wider than long (1.4/0.9), unmodified. Abdomen cylindrical, dorso-posteriorly rounded. Gonopore with six epiandrous spigots (Fig. 31; three males examined). ALS with one widened spigot and one pointed spigot (Fig. 32); PME with two conical spigots (Fig. 32). — CHELICERAE. As in Figs 12–13; with pair of frontal lateral apophyses, each with one modified cone-shaped hair (Figs 33–34); distance between tips of modified hairs: 0.74; without proximal protrusion; frontal face of chelicerae with numerous pores of unknown function (Fig. 35); lateral stridulatory files distinct (Fig. 36), ~70 ridges, distances between ridges proximally ~6 µm, distally ~4 µm. — PALPS. As in Figs 9–11; coxa with rounded retrolateral hump, prolaterally with complex system of comb-shaped processes and long and short hair-like processes (Fig. 37); trochanter barely modified; femur distally widened, with rounded ventral protrusion, dorsally straight, without proximal retrolateral process, with distinct retrolateral transversal line, with prolateral stridulatory pick proximally (Fig. 38); femur–patella joints shifted toward prolateral side; patella



**Figures 5–11.** *Cenemus culiculus* (Simon, 1898), live specimens and male pedipalp. 5–6 Male and female from Mahé, Bel Ombre. 7–8 Female with egg-sac and juvenile male from Mahé, Morne Blanc. 9–11 Left male palp, prolateral, dorsal, and retrolateral views; male from Mahé, Morne Blanc (ZFMK Ar 23868). Abbreviations: co, coxa; fe, femur; gb, genital bulb; pa, patella; pr, procursus; ta, tarsus; ti, tibia; tr, trochanter. Scale bar: 0.5 mm.

triangular in lateral view, i.e. very short ventrally; tibia large compared to femur, tibia-tarsus joints shifted toward retrolateral side; tarsus without macrotrichia, with short dorsal process carrying capsulate tarsal organ (Fig. 39); procursus (Figs 18–20) straight, without ventral “knee”, with dense brush of hairs dorsally and laterally (Fig. 42), proximally without prolateral hump but with ridge, pro-

cursus tip with bifid dorsal sclerite, prolateral tip short and sclerotized, retrolateral tip longer and semitransparent (Fig. 19), procursus tip retrolaterally with small projections around pit with four hair-shaped processes (Fig. 40), ventrally without (or with strongly reduced?) ventral spine; genital bulb (Figs 14–17) with ventral hump, simple basal sclerite connected to distal (main) sclerite; dis-



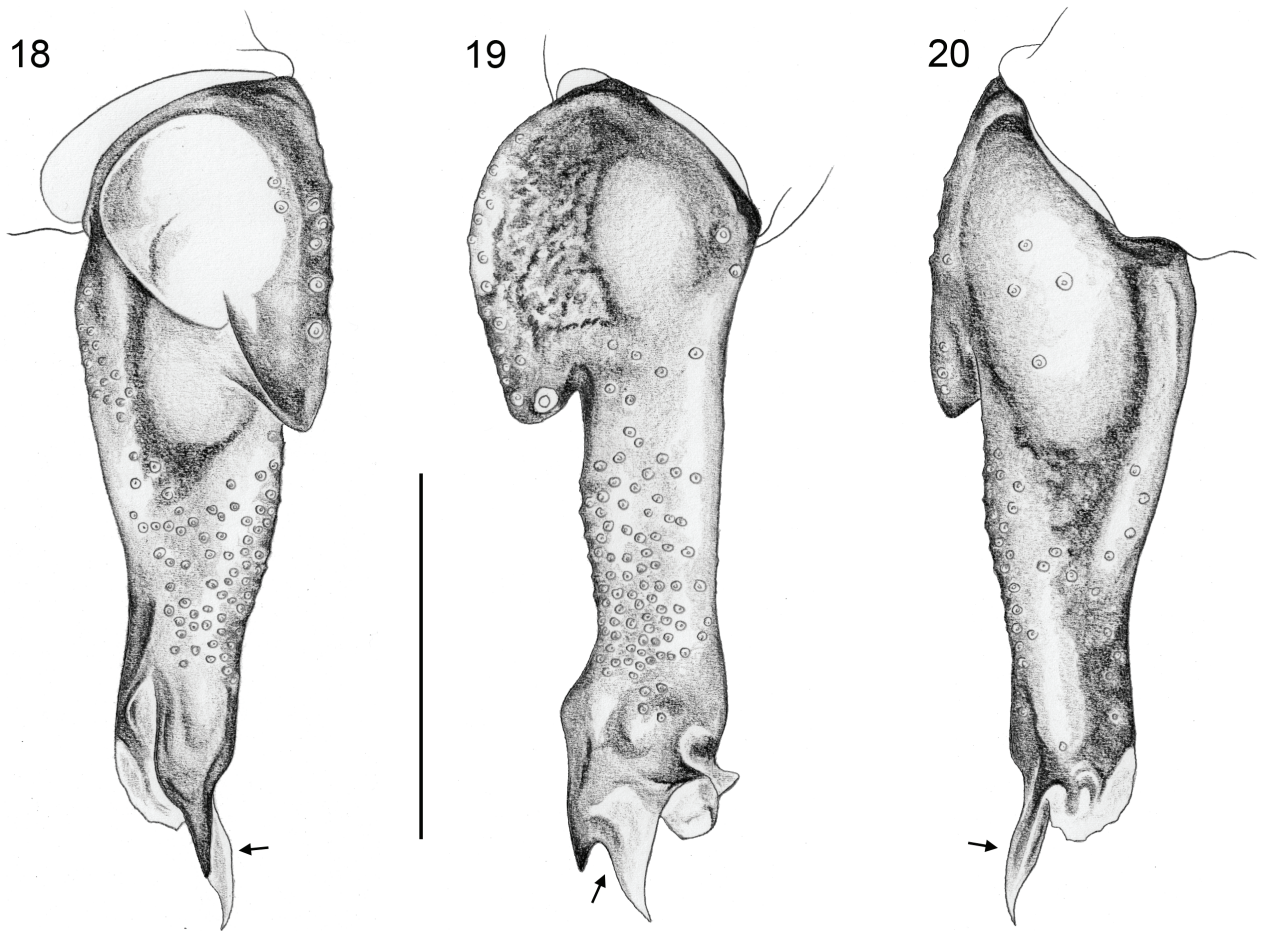
**Figures 12–17.** *Cenemus culiculus* (Simon, 1898); male from Mahé, Morne Blanc (ZFMK Ar 23868). **12–13** Chelicerae, frontal and lateral views. **14–17** Left genital bulb, distal, proterolateral, dorsal, and retrolateral views. Abbreviations: bs, basal sclerite; hu, ventral hump; pp, proterolateral process of distal sclerite; rp, retrolateral process of distal sclerite. Scale bars: 0.5 mm.

tal sclerite with two distinctive processes: short rounded retrolateral process and longer proterolateral process bent at right angle (Figs 43–44), with two transparent processes originating from basis of proterolateral process, possibly extensible and with complex tip (Figs 45–46); sperm duct opening at basis of long proterolateral process (arrows in Figs 43–44). — **LEGS.** Without spines; without curved hairs; few vertical hairs; retrolateral trichobothrium of tibia 1 at 2%; proterolateral trichobothrium absent on tibia 1, present on other tibiae; tarsus 1 with ~35 distinct pseudosegments (cf. female, Fig. 56); tarsal organs capsulate, distinctively oval, with indentation medially on proximal part of rim (cf. female, Figs 58–61).

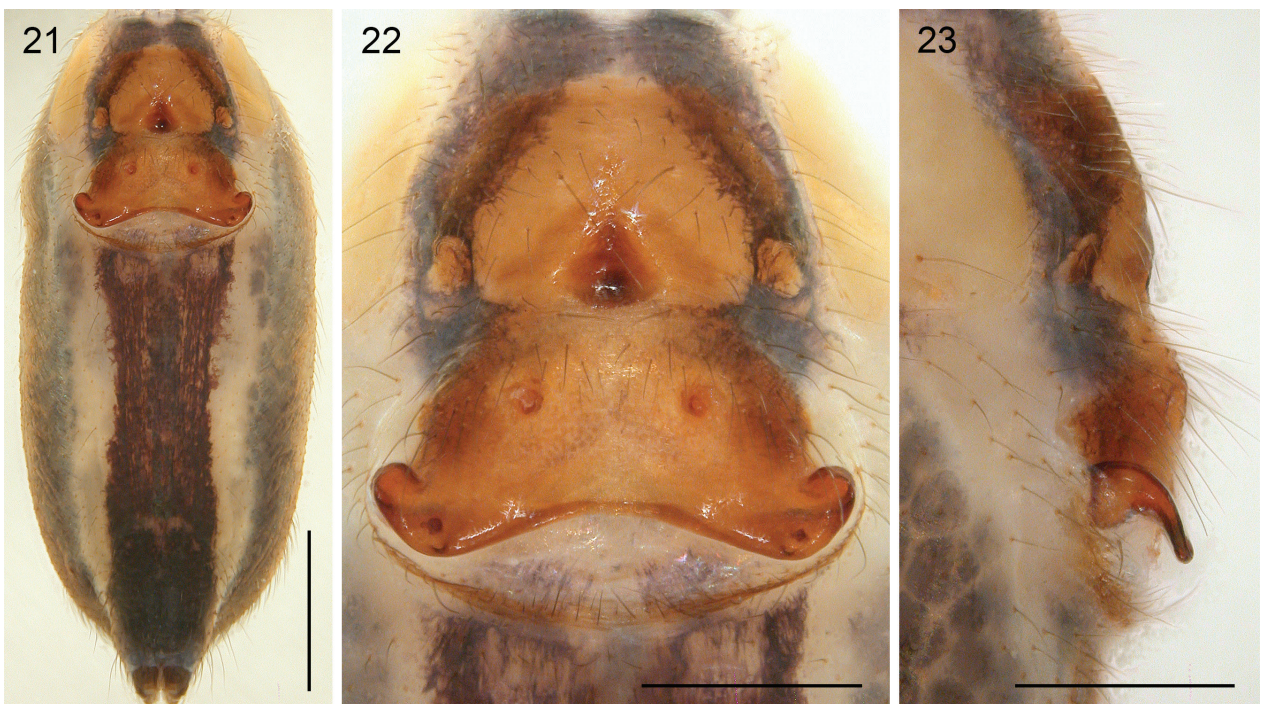
**Variation. Males.** Total body length ~4.0–6.5; tibia 1 in 15 males from Mahé: 10.1–14.5 (mean 12.8); distance between tips of cheliceral apophyses: 0.67–0.76 (N =

14). Sternum sometimes without lateral dark margins; abdomen sometimes also with whitish marks; small males with cheliceral apophyses directed more towards lateral, at up to 40° against vertical line versus 25–30° in large males (i.e., maintaining a similar absolute distance between the tips).

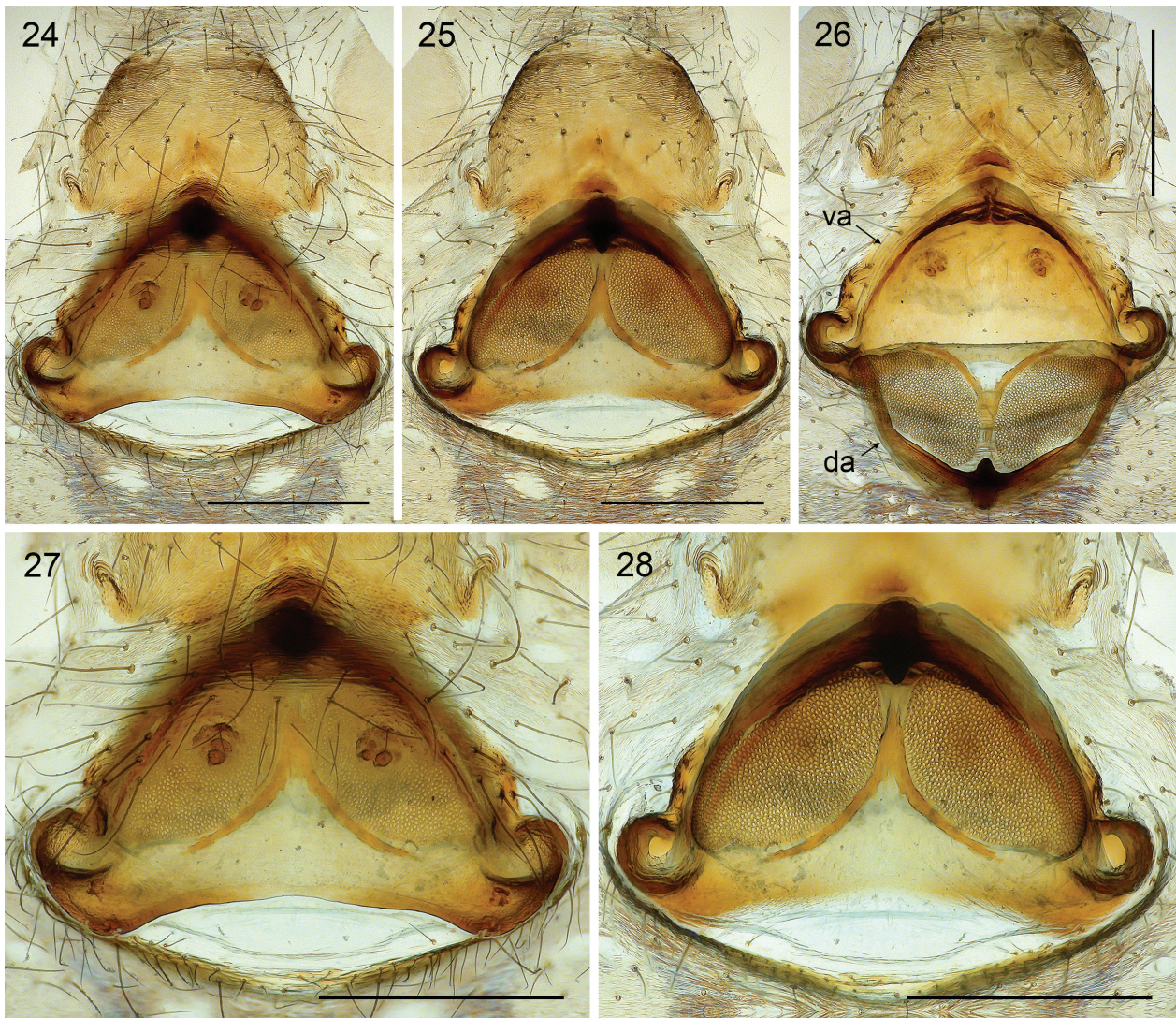
**Female.** In general similar to male (Figs 6–7); ventral abdominal band usually darker and wider than in males (Fig. 21), often divided by light lines into two or three longitudinal bands; cheliceral stridulatory files (Fig. 49) smaller than in males (~40 ridges), distances between ridges proximally ~6 µm, distally ~4.5 µm. Without stridulatory apparatus between carapace and abdomen. Tibia 1 in 20 females from Mahé: 9.2–14.7 (mean 12.6); body length: ~3.5–6.5. Epigynum as in Figs 22–23 and 51–52; main epigynal plate trapezoidal, weakly protrud-



**Figures 18–20.** *Cenemus culiculus* (Simon, 1898); male from Mahé, Morne Blanc (ZFMK Ar 23868); left tarsus and procurus, prolateral, dorsal, and retrolateral views; arrows point at distal dorsal sclerite. Scale bar: 0.5 mm.



**Figures 21–23.** *Cenemus culiculus* (Simon, 1898); female from Mahé, Bel Ombre (ZFMK Ar 23866). **21** Abdomen, ventral view. **22–23** Epigynum, ventral and lateral views. Scale bars: 1 mm (21); 0.5 mm (22–23).



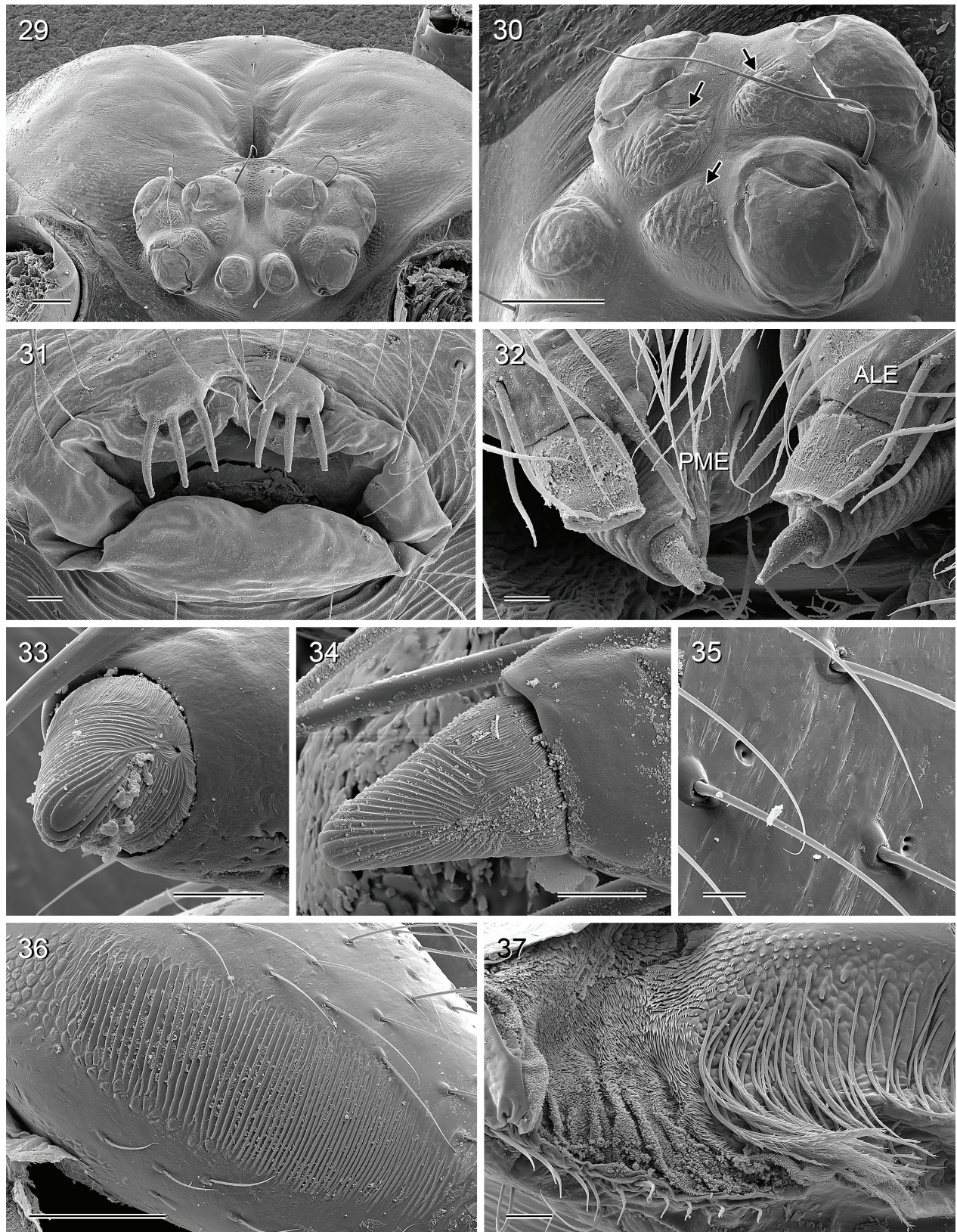
**Figures 24–28.** *Cenemus culiculus* (Simon, 1898); female from Mahé, Morne Blanc (ZFMK Ar 23869). **24–25** Cleared genitalia and anterior plate, ventral and dorsal views. **26** Cleared genitalia, dorsal view, with dorsal arc tilted backwards. **27–28** Cleared genitalia, ventral and dorsal views. Abbreviations: da, dorsal arc; va, ventral arc. Scale bars: 0.5 mm.

ing, only posteriorly laterally with pair of distinctive flat processes, each with small but deep pocket at posterior extreme (arrows in Fig. 52), distances between pockets: 0.60–0.80 (mean 0.70) ( $N = 17$ ); with pair of large pits more anteriorly on main epigynal plate, provided with numerous pores (Fig. 53), distance between pits: 0.27–0.42 (mean 0.34) ( $N = 17$ ); distinct plate in front of epigynum with large dark median pit with smooth cuticle and without pores; posterior epigynal plate short and simple (Fig. 22). Internal genitalia (Figs 24–28) with large oval pore plates converging anteriorly, separated by V-shaped sclerite; dorsal arc with median posterior sclerotized process, ventral arc simple, without ventral median pocket (Fig. 26). Spigots as in male (Figs 62–63).

**Remarks.** The Zoological Museum in Hamburg, Germany, has a further juvenile specimen labeled as holotype (ZMH-A0002275). This specimen seems to originate from the same place and the same collecting event, is very probably conspecific with the MNHN specimen,

and it also fits Simon’s (1898) original description. Simon (1898) did not indicate whether one or two specimens were available to him. We assume that he did not examine the Hamburg specimen, and that it is thus not a type specimen. First, there is no label in Simon’s handwriting with the Hamburg specimen. Second, a label says “Seychellen, A. Brauer leg. 1895, Mus. Marburg, comm. 24. VII. 1901”. The specimen might thus have come to Hamburg directly from Marburg rather than from E. Simon. Unfortunately, the communication from July 1901 is apparently lost (N. Dupérré, personal communication, 12 Nov. 2021).

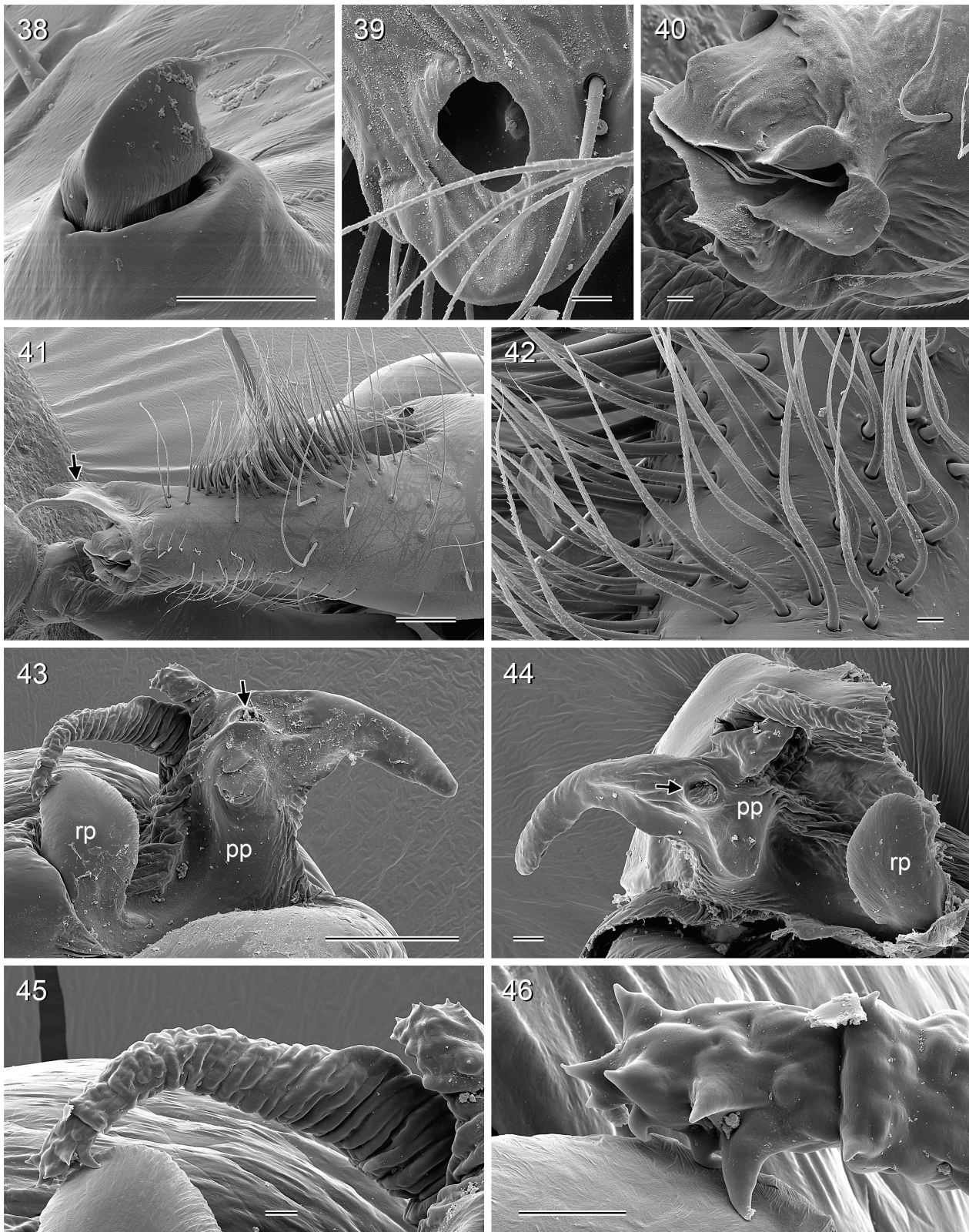
The two specimens (male and female) examined from Silhouette are labeled as *C. culiculus* and originate from the same collecting event as the specimens from Jardin Marron listed in Saaristo (2001) (under *C. culiculus*). The male is extremely similar to specimens from Mahé but has a smaller distance between the tips of the cheliceral apophyses: 0.61. The same is true of the female, which has a smaller distance between the pockets at the posterior epigynal margin: 0.55. In addition, the epigynum



**Figures 29–37.** *Cenemus culiculus* (Simon, 1898); male from Mahé, Morne Blanc (ZFMK Ar 23868). **29** Ocular area and carapace, dorsal-frontal view. **30** Left eye triad and AME, oblique frontal view (arrows: “accessory lenses”). **31** Gonopore. **32** Spinnerets. **33–34** Modified hair on cheliceral apophysis. **35** Pores on frontal cheliceral face. **36** Cheliceral stridulatory file. **37** Palpal coxa (endite), prolateral view. Scale bars: 100  $\mu\text{m}$  (29, 30, 36); 10  $\mu\text{m}$  (31–35); 20  $\mu\text{m}$  (37).

resembles Saaristo’s (2001) drawing of *C. silhouette* rather than his drawing of *C. culiculus*. However, the male bulbal processes appear indistinguishable from those of

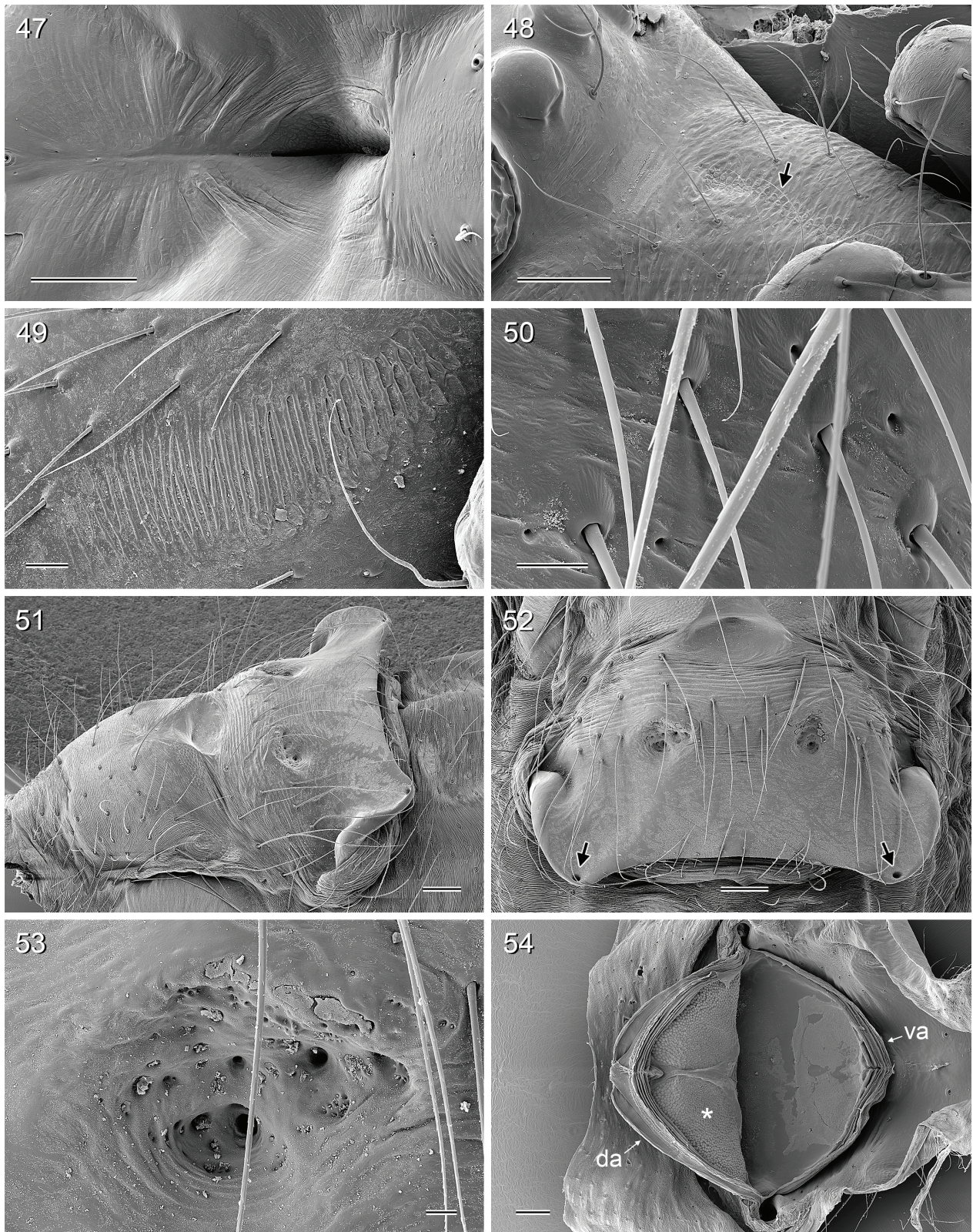
*C. culiculus* from Mahé. In addition, the specimens from Silhouette differ from those of Mahé by a lighter clypeus and a median carapace band that is narrower in the central



**Figures 38–46.** *Cenemus culiculus* (Simon, 1898); male from Mahé, Morne Blanc (ZFMK Ar 23868). **38** Stridulatory pick on palpal femur. **39** Palpal tarsal organ. **40** Procursus tip, ventral part in retrolateral view. **41** Procursus, retrolateral view (arrow: distal dorsal sclerite). **42** Hair-brush on procursus. **43–44** Distal bulbal sclerite (arrows: sperm duct opening). **45** Membranous processes on distal bulbal sclerite. **46** Tip of long membranous processes on distal bulbal sclerite. Abbreviations: pp, prolateral process of distal sclerite; rp, retrolateral process of distal sclerite. Scale bars: 10  $\mu\text{m}$  (38–40, 42, 45, 46); 100  $\mu\text{m}$  (41, 43); 20  $\mu\text{m}$  (44).

part. The assignment of these specimens is thus tentative, and the separation of *C. culiculus* and *C. silhouette* clearly needs further study.

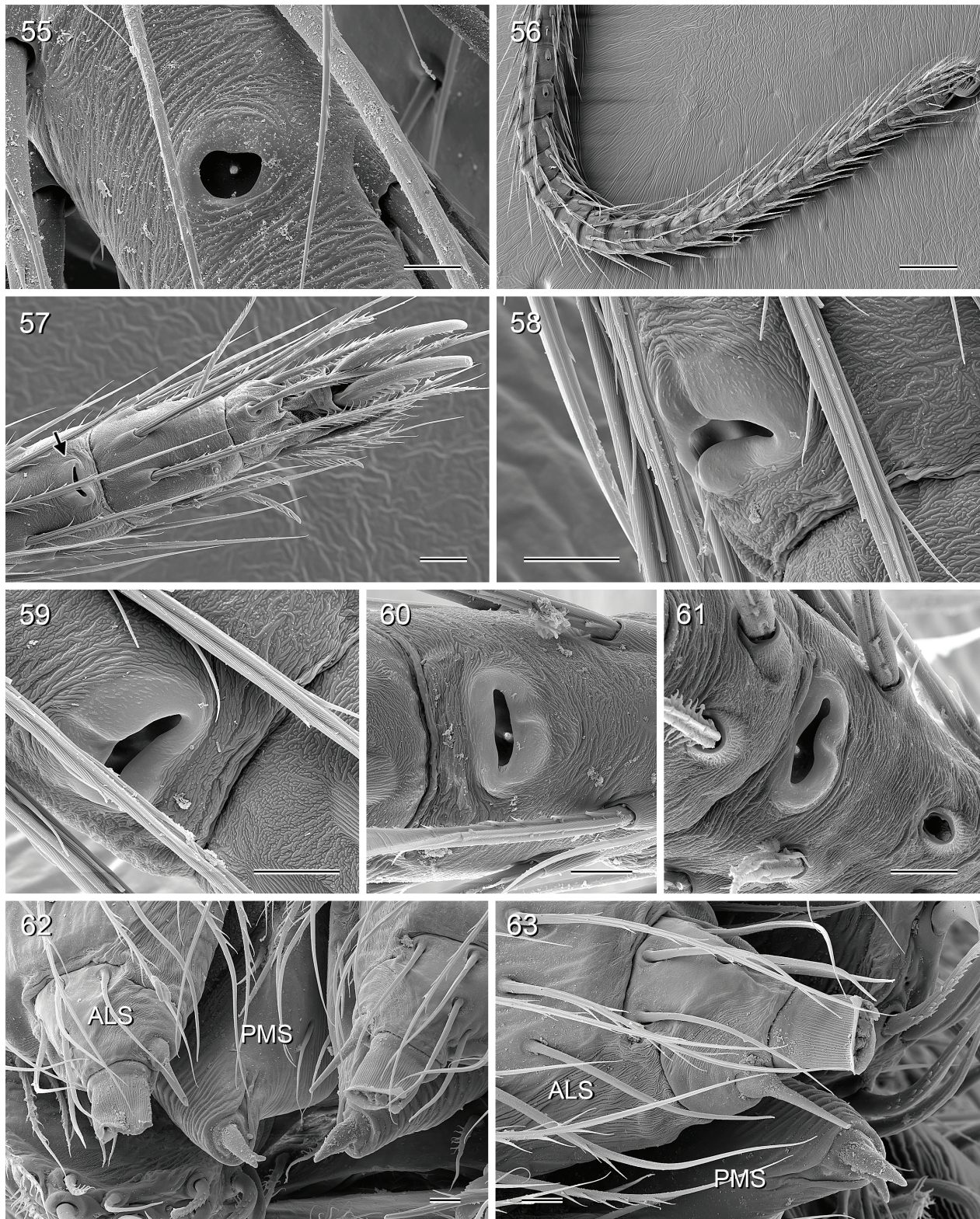
**Natural history.** Adult specimens were mostly found in large sheltered spaces near the ground, between rocks and roots (arrow in Fig. 3). Juveniles often occupied more ex-



**Figures 47–54.** *Cenemus culiculus* (Simon, 1898); female from Mahé, Morne Blanc (ZFMK Ar 23869). **47** Carapace pit. **48** AME and clypeus, oblique frontal view (arrow: modified area). **49** Cheliceral stridulatory file. **50** Pores on frontal cheliceral face. **51** Epigynum and anterior sclerite, lateral-ventral view. **52** Epigynum, ventral view (arrows: pockets). **53** Epigynal pit. **54** Internal female genitalia, dorsal view with dorsal arc tilted toward front (asterisk: pore plate). Abbreviations: da, dorsal arc; va, ventral arc. Scale bars: 100  $\mu\text{m}$  (47, 48, 51, 52, 54); 20  $\mu\text{m}$  (49); 10  $\mu\text{m}$  (50, 53).

posed habitats, among the vegetation up to 2 m above the ground. The domed sheet webs of adults (Fig. 4) had a diameter of ~20–40 cm. No silk balls were seen in the

webs. When disturbed, the spiders tended to run towards the back, i.e. deeper into the shelter, rather than to vibrate or swing their bodies. However, they were often seen to



**Figures 55–63.** *Cenemus culiculus* (Simon, 1898); female from Mahé, Morne Blanc (ZFMK Ar 23869). **55** Palpal tarsal organ. **56** Left tarsus 3, showing distinct pseudosegmentation. **57** Tip of left tarsus 2 (arrow: tarsal organ). **58–59** Tarsal organ on tarsus 1. **60–61** Tarsal organs on tarsi 3 and 4. **62–63** Spinnerets. Scale bars: 10  $\mu\text{m}$  (55, 58–63); 100  $\mu\text{m}$  (56); 20  $\mu\text{m}$  (57).

bob or rotate their abdomens without any obvious disturbance. When caught, they were extremely quick at autotomizing one or more legs.

**Distribution.** Apparently present on Mahé and Silhouette, but see Remarks above.

## 4. Discussion

### 4.1. Morphology

The superficial similarity between *Cenemus* and some representatives of the southern group of Smeringopinae (especially *Smeringopus*) is due to plesiomorphic characters that are shared by *Cenemus* and the southern group. One of them is the relatively long cylindrical abdomen of *Cenemus* that is conspicuously similar to that of most species of *Smeringopus*, but presumably plesiomorphic for Smeringopinae (Huber 2022). It is also similar to the abdomens of some species in the northern group, and does therefore not provide any grouping information. Two further plesiomorphies of *Cenemus* that resemble representatives of the southern group support a basal position of *Cenemus* in the northern group, because *Cenemus* is the only representative in this group that has retained the plesiomorphic condition (Fig. 64). Most conspicuous in this respect are the presence of lateral marks on the carapace and the absence of spines on the male legs. Lateral marks on the carapace are shared with most species of the southern group but do not occur in the northern group except in *Cenemus*. Interestingly, such markings are not present in juvenile specimens of *Cenemus* (Fig. 8; confirmed in five specimens). It is for this reason that they are not mentioned in the original description of the type species (Simon 1898), which is based on a juvenile specimen. The absence of spines on the male legs is also shared by *Cenemus* and the southern group, while all representatives of the northern group except for *Cenemus* have such spines (usually on femur 1, very rarely also on tibia 1 and femur 2). A further plesiomorphy is shared between *Cenemus* and all other representatives of the northern group, and does therefore not provide any grouping information for *Cenemus*: the presence of cheliceral stridulatory files. Finally, *Cenemus* is the only representative of Smeringopinae that has retained the plesiomorphic condition of distinct tarsal pseudosegments. All other Smeringopinae are characterized by an indistinct pseudosegmentation, with irregular cuticular platelets rather than regular rings (Huber 2012, 2013, 2020, 2022; Huber et al. 2021).

In contrast to most of the characters listed above, the two morphological synapomorphies that support the inclusion of *Cenemus* in the northern group (Fig. 64) are rather inconspicuous, i.e. require strong magnification or SEM. (1) Reduced number of spigots on the anterior lateral spinnerets. All representatives of the southern group have retained the plesiomorphic set of seven to eight spigots on each side, while *Cenemus* and all other representatives of the northern group have a reduced set of only two spigots. (2) Tendency to increase the number of epiandrous spigots. The plesiomorphic condition is the presence of four epiandrous spigots. *Cenemus* and many other representatives of the northern group share an increase of spigot numbers up to eight. By contrast, all members of the southern group share a reduction of epiandrous spigots to two.

Finally, the unique shape of the leg tarsal organ of *Cenemus* is certainly derived but not shared by any other genus in Pholcidae and thus phylogenetically uninformative at genus level.

### 4.2. Smeringopinae phylogeny and the age of *Cenemus*

Our data strongly support the inclusion of *Cenemus* in the northern group of Smeringopinae, rather than in the Sub-Saharan southern group. This suggests that the genus dates back to a period between the separation of the Mascarene platform from Madagascar (~85 mya) and its separation from India (~60 mya). *Cenemus* thus joins the long list of endemic Seychellois genera that are thought to be relicts from the breakup of Gondwana (Stoddart 1984). In addition, these numbers provide valuable additional calibration points for dating the pholcid tree of life. This has been notoriously difficult due to the paucity of suitable fossils in Pholcidae (Dimitrov et al. 2012; Eberle et al. 2018).

Beyond the position of *Cenemus* in the northern group of Smeringopinae, our molecular data are partly difficult to reconcile with morphological evidence. Figure 64 illustrates the conflicting details. While the available morphological evidence is most easily explained by a sister-group relationship between *Cenemus* and all other representatives of the northern group of Smeringopinae, molecules suggest that *Holocnemus pluchei* + *Hoplopholcus* are even more “basal” in this group. We suspect that the *Holocnemus pluchei* sequences we used may at least partly cause this problem. Several previous molecular studies have encountered problems with this particular species (Bruvo-Madžarić et al. 2005; Astrin et al. 2007; Eberle et al. 2018). In our analyses, *Holocnemus pluchei* is the only taxon of the northern group that is in some cases placed in the southern group, as sister to Central African *Smeringopus*, a quite obvious misplacement.

Other than the position of *Cenemus*, a few further results of the phylogenetic analyses are noteworthy. All of them concern the northern group (our results regarding the southern group do not differ in any fundamental way from those in Eberle et al. 2018, which is unsurprising as we used the same taxa and genes). First, all analyses agree with respect to the sister group relationship between *Crossopriza* and *Maghreba*, with high support values. *Maghreba* was not included in the molecular phylogeny of Eberle et al. (2018), and the most recent morphological cladistic analysis (Huber 2022) remained vague about the relationships between *Crossopriza*, *Maghreba*, *Stygopholcus*, and *Holocnemus hispanicus*. Thus, even though based on a limited gene sampling, this sister group relationship between *Crossopriza* and *Maghreba* is plausible. Second, all analyses agree with respect to the non-monophyly of *Holocnemus* as currently construed. This is in exact agreement with the recent morphological analysis (Huber 2022) that also separated *Holocnemus* into three clades, none of which are connected by a sister group relationship: the type species *H. pluchei*; the Iberian *H. his-*

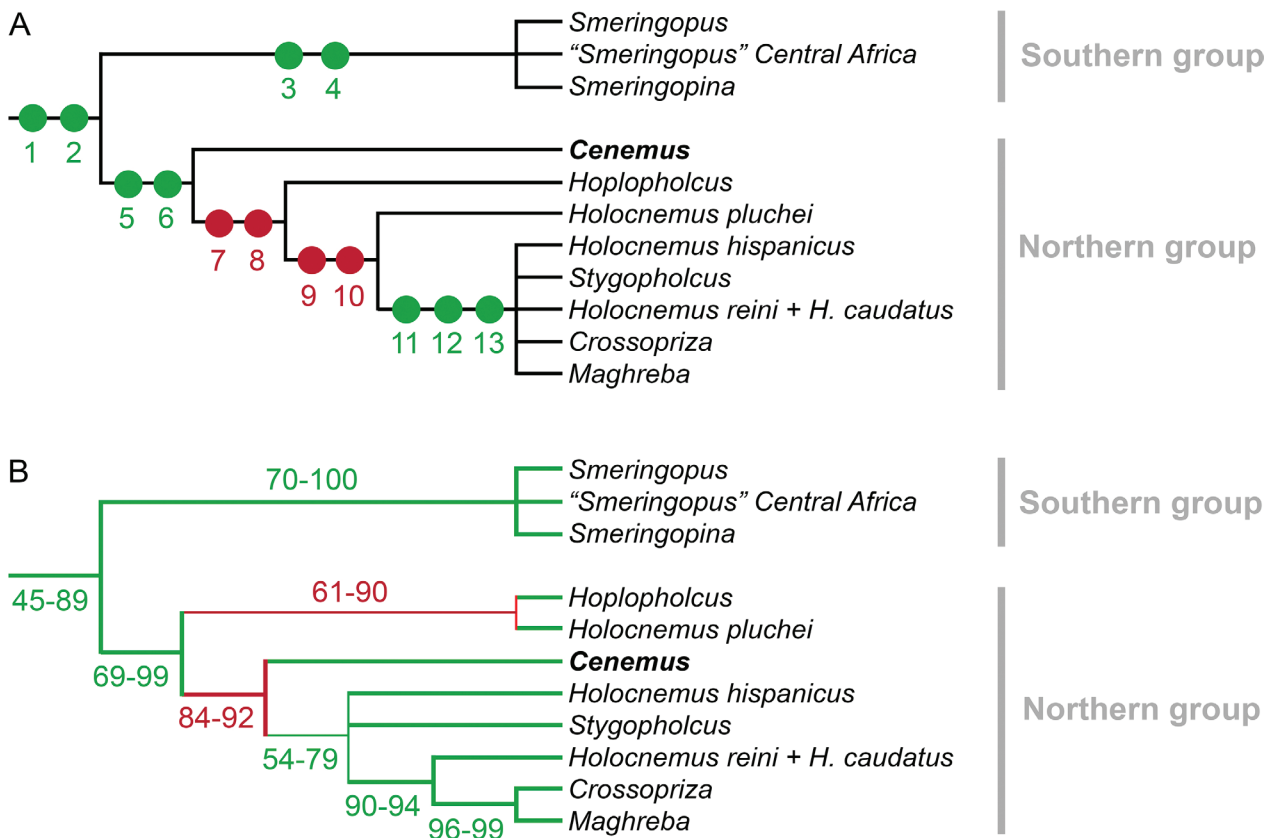


**Figure 64.** Overview of putative Smeringopinae relationships, showing the main conflicts (red) between morphological (A) and molecular (B) evidence. **A** Morphological and karyological support for each node, mapped on a hybrid tree derived from cladistic analysis (Huber 2022) and manual placement of *Cenemus*; character information from Ávila-Herrera et al. (2021), Dederichs et al. (2022); Huber (2012, 2013, 2020, 2022), Huber et al. (2021), and present paper. Characters: 1, large and deep thoracic pit; 2, sperm with microtubules in implantation fossa; 3, reduction of cheliceral stridulation; 4, reduction of epiandrous spigots from four to two; 5, tendency of increase of epiandrous spigots to more than four; 6, reduction of ALS spigots to two on each side; 7, reduction of lateral carapace marks; 8, spines on male anterior legs; 9, spots on legs; 10, change from  $X_1X_20$  to  $X0$  karyotype system; 11, reduction of 13 to 11 chromosome pairs; 12, nucleolus organizer region at end of single X chromosome; 13, abdomen posteriorly dorsally angular to pointed. **B** Molecular support (UFBoot in %) for individual nodes, taken from the 16 trees without obvious misplacements (Pholcinae monophyletic; Smeringopinae monophyletic; *Holocnemus plucei* in northern group; all *Smeringopus* in southern group). Thick lines: mostly high (>80) support; thin lines: mostly low (<80) support. Nodes with low support are collapsed unless supported by morphology.

*panicus*; and the two closely related *H. reini* + *H. caudatus* (the latter species is not included in the present analyses but it shares two unique synapomorphies with *H. reini*, see Huber 2022). Third, all analyses agree with respect to a “basal” position of *Hoplopholcus* within the northern group; this is in agreement with both the molecular analysis in Eberle et al. (2018) and with the most recent morphological analysis (Huber 2022). This is remarkable because it further strengthens the idea that *Hoplopholcus* and *Stygopholcus*, two superficially very similar (compare Fig. 1B and D) and geographically neighboring genera, are not sister taxa and not even paraphyletic.

#### 4.3. Male-female covariation and species limits

Species limits are not the focus of this paper because fresh material was only available of the type species. However, there seems to be a functional correlation between the

male cheliceral apophyses and the marginal pockets on the female epigynum and this might be useful for future analyses of species limits. An interaction between these male and female structures during copulation seems to be very widespread in Pholcidae (Kraus 1984; Huber 2003, 2005, 2022) and our measurements above suggest the same for *Cenemus*: the specimens from Silhouette Island had smaller values for both distances than the Mahé specimens. This allows a prediction about the unknown male of *C. mikehilli*, a species in which the female pockets are particularly wide apart: the male is predicted to have strongly diverging cheliceral apophyses.

## 5. Conclusion

The morphology of the endemic Seychellois genus *Cenemus* Saaristo, 2001 is characterized by numerous ple-

siomorphies, suggesting a “basal” position within the northern group of Smeringopinae. Our new molecular data support this idea, even though there remains conflict regarding the exact sister group. The position of *Cenemus* within the northern group of Smeringopinae (Mediterranean to India) rather than in the Subsaharan southern group indicates that *Cenemus* dates back to the breakup of Gondwana, between the separation of the Mascarene platform from Madagascar (~85 mya) and its separation from India (~60 mya). This publication terminates a series of papers on the Pholcidae subfamily Smeringopinae (Huber 2012, 2013, 2020, 2022; Huber et al. 2021).

## 6. Acknowledgements

We thank J. Gerlach for help with previously published localities; N. Dupérré for information on the supposed holotype of *C. culiculus* in the Hamburg museum; C. Hoareau for donating specimens; C. Eitzbauer and L. Podsiadlowski for support in the molecular lab; R. Victor, I. Al Zakwani, and H. Belhadj for help with the preparation of collecting trips, with permits, and logistics; and S. Benjamin and C. Haddad for helpful comments on the manuscript.

## 7. References

- Aberer AJ, Krompass D, Stamatakis A (2013) Pruning rogue taxa improves phylogenetic accuracy: an efficient algorithm and webserver. *Systematic Biology* 62: 162–166. <https://doi.org/10.1093/sysbio/sys078>
- Astrin JJ, Misof B, Huber BA (2007) The pitfalls of exaggeration: molecular and morphological evidence suggests *Kaliana* is a synonym of *Mesabolivar* (Araneae: Pholcidae). *Zootaxa* 1646: 17–30. <https://doi.org/10.11646/zootaxa.1646.1.2>
- Astrin JJ, Höfer H, Spelda J, Holstein J, Bayer S, Hendrich L, Huber BA, Kielhorn K-H, Krammer H-J, Lemke M, Monje JC, Morinière J, Rulik B, Petersen M, Janssen H, Muster C (2016) Towards a DNA barcode reference database for spiders and harvestmen of Germany. *PLoS One* 11(9): e0162624. <https://doi.org/10.1371/journal.pone.0162624>
- Brignoli PM (1981) Studies on the Pholcidae, I. Notes on the genera *Artema* and *Physocyclus* (Araneae). *Bulletin of the American Museum of Natural History* 170(1): 90–100.
- Brown BV (1993) A further chemical alternative to critical-point-drying for preparing small (or large) flies. *Fly Times* 11: 10.
- Bruvo-Madarić B, Huber BA, Steinacher A, Pass G (2005) Phylogeny of pholcid spiders (Araneae: Pholcidae): combined analysis using morphology and molecules. *Molecular Phylogenetics and Evolution* 37: 661–673. <http://dx.doi.org/10.1016/j.ympev.2005.08.016>
- Capella-Gutiérrez S, Silla-Martínez JM, Gabaldón T (2009) trimAl: a tool for automated alignment trimming in large-scale phylogenetic analyses. *Bioinformatics* 25: 1972–1973. <https://doi.org/10.1093/bioinformatics/btp348>
- Cock PJ, Antao T, Chang JT, Chapman BA, Cox CJ, Dalke A, Friedberg I, Hamelryck T, Kauff F, Wilczynski B, de Hoon MJ (2009) Biopython: freely available Python tools for computational molecular biology and bioinformatics. *Bioinformatics* 25: 1422–1423. <https://doi.org/10.1093/bioinformatics/btp163>
- Cogan BH (1984) Origins and affinities of Seychelles insect fauna. In: Stoddart DR (Ed.) *Biogeography and Ecology of the Seychelles Islands*. Monographiae Biologicae 55. Junk, The Hague, 245–258.
- Collier JS, Sansom V, Ishizuka O, Taylor RN, Minshull TA, Whitmarsh RB (2008) Age of Seychelles-India break-up. *Earth and Planetary Science Letters* 272: 264–277. <https://doi.org/10.1016/j.epsl.2008.04.045>
- Dederichs TM, Huber BA, Michalik P (2022) Evolutionary morphology of sperm in pholcid spiders (Pholcidae, Synspermiata). *BMC Zoology* 7: 52. <https://doi.org/10.1186/s40850-022-00148-3>
- Dimitrov D, Arnedo MA, Ribera C (2008) Colonization and diversification of the spider genus *Pholcus* Walckenaer, 1805 (Araneae, Pholcidae) in the Macaronesian archipelagos: Evidence for long-term occupancy yet rapid speciation. *Molecular Phylogenetics and Evolution* 48: 596–614. <https://doi.org/10.1016/j.ympev.2008.04.027>
- Eberle J, Dimitrov D, Valdez-Mondragón A, Huber BA (2018) Microhabitat change drives diversification in pholcid spiders. *BMC Evolutionary Biology* 18: 141. <https://doi.org/10.1186/s12862-018-1244-8>
- Guindon S, Dufayard J-F, Lefort V, Anisimova M, Hordijk W, Gascuel O (2010) New algorithms and methods to estimate maximum-likelihood phylogenies: assessing the performance of PhyML 3.0. *Systematic Biology* 59: 307–321. <https://doi.org/10.1093/sysbio/syq010>
- Huber BA (2000) New World pholcid spiders (Araneae: Pholcidae): a revision at generic level. *Bulletin of the American Museum of Natural History* 254: 1–348. [https://doi.org/10.1206/0003-0090\(2000\)254<0001:NWPSAP>2.0.CO;2](https://doi.org/10.1206/0003-0090(2000)254<0001:NWPSAP>2.0.CO;2)
- Huber BA (2003) Southern African pholcid spiders: revision and cladistic analysis of *Quamtana* gen. nov. and *Spermophora* Hentz (Araneae: Pholcidae), with notes on male-female covariation. *Zoological Journal of the Linnean Society* 139: 477–527. <http://dx.doi.org/10.1046/j.0024-4082.2003.00082.x>
- Huber BA (2005) High species diversity, male-female coevolution, and metaphyly in Southeast Asian pholcid spiders: the case of *Belisana* Thorell 1898 (Araneae, Pholcidae). *Zoologica* 155: 1–126.
- Huber BA (2007) Two new genera of small, six-eyed pholcid spiders from West Africa, and first record of *Spermophorides* for mainland Africa (Araneae: Pholcidae). *Zootaxa* 1635: 23–43. <https://doi.org/10.11646/zootaxa.1635.1.2>
- Huber BA (2012) Revision and cladistic analysis of the Afrotropical endemic genus *Smeringopus* Simon, 1890 (Araneae: Pholcidae). *Zootaxa* 3461: 1–138. <https://doi.org/10.11646/zootaxa.3461.1.1>
- Huber BA (2013) Revision and cladistic analysis of the Guineo-Congolian spider genus *Smeringopina* Kraus (Araneae, Pholcidae). *Zootaxa* 3713: 1–160. <http://dx.doi.org/10.11646/zootaxa.3713.1.1>
- Huber BA (2020) Revision of the spider genus *Hoplopholcus* Kulczyński (Araneae, Pholcidae). *Zootaxa* 4726: 1–94. <https://doi.org/10.11646/zootaxa.4726.1.1>
- Huber BA (2022) Revisions of *Holocnemus* and *Crossopriza*: the spotted-leg clade of Smeringopinae (Araneae, Pholcidae). *European Journal of Taxonomy* 795: 1–241. <https://doi.org/10.5852/ejt.2022.795.1663>
- Huber BA, Carvalho LS (2019) Filling the gaps: descriptions of unnamed species included in the latest molecular phylogeny of Pholcidae (Araneae). *Zootaxa* 4546: 1–96. <https://doi.org/10.11646/zootaxa.4546.1.1>
- Huber BA, Fischer N, Astrin JJ (2010) High level of endemism in Haiti’s last remaining forests: a revision of *Modisimus* (Araneae: Pholcidae) on Hispaniola, using morphology and molecules. *Zoo-*

- logical Journal of the Linnean Society 158: 244–299. <http://dx.doi.org/10.1111/j.1096-3642.2009.00559.x>
- Huber BA, Neumann J, Grabolle A, Hula V (2017) Aliens in Europe: updates on the distributions of *Modisimus culicinus* and *Micropholcus fauroti* (Araneae, Pholcidae). *Arachnologische Mitteilungen* 53: 12–18. <http://doi.org/10.5431/aramit5303>
- Huber BA, Eberle J, Dimitrov D (2018) The phylogeny of pholcid spiders: a critical evaluation of relationships suggested by molecular data (Araneae, Pholcidae). *ZooKeys* 789: 51–101. <http://doi.org/10.3897/zookeys.789.22781>
- Huber BA, Pavlek M, Komnenov M (2021) Revision of the spider genus *Stygopholcus* (Araneae, Pholcidae), endemic to the Balkan Peninsula. *European Journal of Taxonomy* 752: 1–60. <https://doi.org/10.5852/ejt.2021.752.1391>
- Huber BA, Meng G, Acurio AE, Astrin JJ, Inclán DJ, Izquierdo M, Valdez-Mondragón A (2022) *Metagonia* spiders of Galápagos: blind cave-dwellers and their epigean relatives (Araneae, Pholcidae). *Invertebrate Systematics* 36: 647–678. <https://doi.org/10.1071/IS21082>
- Junier T, Zdobnov EM (2010) The Newick utilities: high-throughput phylogenetic tree processing in the UNIX shell. *Bioinformatics* 26: 1669–1670. <https://doi.org/10.1093/bioinformatics/btq243>
- Kalyaanamoorthy S, Minh BQ, Wong TKF, von Haeseler A, Jermini LS (2017) ModelFinder: fast model selection for accurate phylogenetic estimates. *Nature Methods* 14: 587–589. <https://doi.org/10.1038/nmeth.4285>
- Katoh K, Standley DM (2013) MAFFT multiple sequence alignment software version 7: improvements in performance and usability. *Molecular Biology and Evolution* 30: 772–780. <https://doi.org/10.1093/molbev/mst010>
- Kearse M, Moir R, Wilson A, Stones-Havas S, Cheung M, Sturrock S, Buxton S, Cooper A, Markowitz S, Duran C, Thierer T, Ashton B, Meintjes P, Drummond A (2012) Geneious Basic: An integrated and extendable desktop software platform for the organization and analysis of sequence data. *Bioinformatics* 28: 1647–1649. <https://doi.org/10.1093/bioinformatics/bts199>
- Kraus O (1984) Male spider genitalia: evolutionary changes in structure and function. *Verhandlungen des Naturwissenschaftlichen Vereins in Hamburg (NF)* 27: 373–382.
- Kück P, Longo GC (2014) FASconCAT-G: extensive functions for multiple sequence alignment preparations concerning phylogenetic studies. *Frontiers in Zoology* 11: 81. <https://doi.org/10.1186/s12983-014-0081-x>
- Letunic I, Bork P (2021) Interactive Tree Of Life (iTOL) v5: an online tool for phylogenetic tree display and annotation. *Nucleic Acids Research* 49: W293–W296. <https://doi.org/10.1093/nar/gkab301>
- Minh BQ, Nguyen MAT, von Haeseler A (2013) Ultrafast approximation for phylogenetic bootstrap. *Molecular Biology and Evolution* 30: 1188–1195. <https://doi.org/10.1093/molbev/mst024>
- Minh BQ, Schmidt HA, Chernomor O, Schrempf D, Woodhams MD, von Haeseler A, Lanfear R (2020) IQ-TREE 2: New models and efficient methods for phylogenetic inference in the genomic era. *Molecular Biology and Evolution* 37: 1530–1534. <https://doi.org/10.1093/molbev/msaa015>
- Nussbaum RA (1984) Amphibians of the Seychelles. In: Stoddart DR (Ed.) *Biogeography and Ecology of the Seychelles Islands. Monographiae Biologicae* 55. Junk, The Hague, 379–415.
- Procter J (1984) Floristics of the granitic islands of the Seychelles. In: Stoddart DR (Ed.) *Biogeography and Ecology of the Seychelles Islands. Monographiae Biologicae* 55. Junk, The Hague, pp. 209–220.
- Ratnasingham S, Hebert PDN (2007) bold: The Barcode of Life Data System (<http://www.barcodinglife.org>). *Molecular Ecology Notes* 7: 355–364. <https://dx.doi.org/10.1111%2Fj.1471-8286.2007.01678.x>
- Saaristo MI (1978) Spiders (Arachnida, Araneae) from the Seychelle islands, with notes on taxonomy. *Annales Zoologici Fennici* 15: 99–126.
- Saaristo MI (1999) An arachnological excursion to the granitic Seychelles, 1–26th January 1999. *Arachnid species lists for Silhouette, Cousine & Mahé. Phelsuma* 7 (suppl.): 1–12.
- Saaristo MI (2001) Pholcid spiders of the granitic Seychelles (Araneae, Pholcidae). *Phelsuma* 9: 9–28.
- Saaristo MI (2002) New species and interesting new records of spiders from Seychelles (Arachnida, Araneae [sic]). *Phelsuma* 10 (suppl. A): 1–31.
- Saaristo MI (2010) Araneae. In: Gerlach J, Marusik YM (Eds) *Arachnida and Myriapoda of the Seychelles islands*. Siri Scientific Press, Manchester, 8–306.
- Sanderson MJ, Shaffer HB (2002) Troubleshooting molecular phylogenetic analyses. *Annual Review of Ecology and Systematics* 33: 49–72. <https://doi.org/10.1146/annurev.ecolsys.33.010802.150509>
- Simon E (1898) *Etudes arachnologiques. 29e Mémoire. XLVI. Arachnides recueillis en 1895 par M. le Dr A. Brauer (de l'Université de Marburg) aux îles Séchelles*. *Annales de la Société Entomologique de France* 66: 370–388.
- Srivathsan A, Lee L, Katoh K, Hartop E, Kutty SN, Wong J, Yeo D, Meier R (2021) ONTbarcoder and MinION barcodes aid biodiversity discovery and identification by everyone, for everyone. *BMC Biology* 19: 217. <https://doi.org/10.1186/s12915-021-01141-x>
- Stamatakis A (2014) RAxML version 8: a tool for phylogenetic analysis and post-analysis of large phylogenies. *Bioinformatics* 30: 1312–1313. <https://doi.org/10.1093/bioinformatics/btu033>
- Steenwyk JL, Buida III TJ, Li Y, Shen X-X, Rokas A (2020) ClipKIT: A multiple sequence alignment trimming software for accurate phylogenomic inference. *PLoS Biology* 18: e3001007. <https://doi.org/10.1371/journal.pbio.3001007>
- Stoddart DR (1984) *Biogeography and Ecology of the Seychelles Islands. Monographiae Biologicae* 55. Junk, The Hague, 692 pp.
- Suyama M, Torrents D, Bork P (2006) PAL2NAL: robust conversion of protein sequence alignments into the corresponding codon alignments. *Nucleic Acids Research* 34: W609–W612. <https://doi.org/10.1093/nar/gkl315>
- Tabei Y, Kiryu H, Kin T, Asai K (2008) A fast structural multiple alignment method for long RNA sequences. *BMC Bioinformatics* 9: 33. <https://doi.org/10.1186/1471-2105-9-33>
- Talavera G, Castresana J (2007) Improvement of phylogenies after removing divergent and ambiguously aligned blocks from protein sequence alignments. *Systematic Biology* 56: 564–577. <https://doi.org/10.1080/10635150701472164>
- Truett G, Heeger P, Mynatt R, Truett A, Walker J, Warman MJB (2000) Preparation of PCR-quality mouse genomic DNA with hot sodium hydroxide and tris (HotSHOT). *Biotechniques* 29: 52–54. <https://doi.org/10.2144/00291bm09>
- Valdez-Mondragón A (2013) Morphological phylogenetic analysis of the spider genus *Physocyclus* (Araneae: Pholcidae). *Journal of Arachnology* 41: 184–196. <https://doi.org/10.1636/K12-33.1>
- Wallace AR (1880) *Island Life*. Macmillan and Co., London. I–xvii + 526 pp.
- Wheeler WC, Coddington JA, Crowley LM, Dimitrov D, Goloboff PA, Griswold CE, Hormiga G, Prendini L, Ramírez MJ, Sierwald P, Almeida-Silva L, Alvarez-Padilla F, Arnedo MA, Benavides Silva

- LR, Benjamin SP, Bond JE, Grismado CJ, Hasan E, Hedin M, Izquierdo MA, Labarque FM, Ledford J, Lopardo L, Maddison WP, Miller JA, Piacentini LN, Platnick NI, Polotow D, Silva-Dávila D, Scharff N, Szűts T, Ubick D, Vink CJ, Wood HM, Zhang J (2017) The spider tree of life: phylogeny of Araneae based on target-gene analyses from an extensive taxon sampling. *Cladistics* 33: 574–616. <https://doi.org/10.1111/cla.12182>
- Yang C, Zheng Y, Tan S, Meng G, Rao W, Yang C, Bourne DG, O'Brien PA, Xu J, Liao S, Chen A, Chen X, Jia X, Zhang A, Liu S (2020) Efficient COI barcoding using high throughput single-end 400 bp sequencing. *BMC Genomics* 21: 862. <https://doi.org/10.1186/s12864-020-07255-w>
- Yao Z, Dong T, Zheng G, Fu J, Li S (2016) High endemism at cave entrances: a case study of spiders of the genus *Uthina*. *Scientific Reports* 6:35757: 1–9, suppl. 1–52. <https://doi.org/10.1038/srep35757>
- Zhang C, Rabiee M, Sayyari E, Mirarab S (2018) ASTRAL-III: polynomial time species tree reconstruction from partially resolved gene trees. *BMC Bioinformatics* 19 (S6): 153. <https://doi.org/10.1186/s12859-018-2129-y>

## Appendix 1

### Annotated list of the Pholcidae of the Seychelles

Twelve species of Pholcidae have been recorded from the Seychelles. At least eight of these are introduced species, most of which have followed humans around the globe. The only certain native species are the three representatives of *Cenemus*. The status (native or introduced) of the twelfth species, *Spermophorides lascars*, is unclear.

#### A1.1. *Artema atlanta* Walckenaer, 1837

**Remarks.** Introduced pantropical species; origin probably Middle East (Huber and Carvalho 2019). Only one previous record from the Seychelles (Saaristo 2001: Silhouette, La Passe; “well established colony”).

**New record** [origin according to label uncertain]. SEYCHELLES – **Aldabra Atoll** • 1 ♀; Isle Picard; 9.401°S, 46.206°E; 25 Mar. 1985; P. Mundel leg.; USNM.

#### A1.2. *Cenemus culiculus* (Simon, 1898)

**Remarks.** Endemic species known from Mahé and Silhouette; separation from *C. silhouette* needs further study (see main text).

#### A1.3. *Cenemus mikehilli* Saaristo, 2002

**Remarks.** Endemic species known from two female specimens only, originating from Marianne and La Digue, respectively (Saaristo 2002).

#### A1.4. *Cenemus silhouette* Saaristo, 2001

**Remarks.** Endemic species known from Silhouette only; separation from *C. culiculus* needs further study (see main text).

#### A1.5. *Crossopriza lyoni* (Blackwall, 1867)

**Remarks.** This pantropical spider has only recently been recorded from the Seychelles (Huber 2022: Mahé); origin probably Middle East or central Asia (Huber 2022).

#### A1.6. *Micropholcus fauroti* (Simon, 1887)

**Remarks.** Pantropical spider introduced to the Seychelles; origin unclear, possibly Middle East (judging from undescribed species from the Arabian Peninsula; B.A. Huber unpubl. data). Numerous records from several islands (Saaristo 2001 and references therein).

#### A1.7. *Modisimus culicinus* (Simon, 1893)

**Remarks.** Pantropical spider introduced to the Seychelles; origin Central America or Caribbean (Huber et al. 2017). Numerous records from several islands (Saaristo 2001 and references therein).

#### A1.8. *Physocyclus globosus* (Taczanowski, 1874)

**Remarks.** Pantropical spider introduced to the Seychelles; origin North or Central America (Brignoli 1981; Valdez-Mondragón 2013). Several records from Mahé, Cousine, and Silhouette (Saaristo 1999, 2001).

**New records.** SEYCHELLES – **Aldabra Atoll** • 1 ♂, 1 ♀; Isle Picard; 9.401°S, 46.206°E; 14 Mar. 1985; P. Mundel & Philip leg.; USNM • 2 ♂♂, 4 ♀♀; Isle Picard; 9.401°S, 46.206°E; 12 Mar. 1985; P. Mundel & Philip leg.; USNM.

#### A1.9. *Smeringopus pallidus* (Blackwall, 1858)

**Remarks.** Pantropical spider introduced to the Seychelles; origin eastern Africa (Huber 2012). Numerous

records from several islands (Saaristo 2001 and references therein).

**New records.** SEYCHELLES – **Mahé** • 1 ♂; Port Glaud, near Cap Ternay; 4.6452°S, 55.3883°E; 40 m a.s.l.; 4 Mar. 2013; C. Hoareau leg.; ZFMK Ar 23927 • 1 ♂, 1 ♀; Baie Lazare; 4.7562°S, 55.4732°E; 25 m a.s.l.; 5 Mar. 2013; C. Hoareau leg.; ZFMK Ar 23928 – **La Digue** • 2 ♀♀; La Digue; 4.36°S, 55.84°E; 8 May 1979; Walch, Löffler, Ackermann & Weigelt leg.; sand beach; SMF • 3 ♀♀, several juveniles; La Digue; 4.36°S, 55.84°E; 17 May 1979; Walch, Löffler, Ackermann & Weigelt leg.; walls, palm and broadleaf forest; SMF – **Praslin** • 3 ♀♀; Pasquere; 4.314°S, 55.721°E; 26 Jan. 1958; H.W Joubert leg.; USNM – **Aldabra Atoll** • 1 ♀; Isle Picard; 9.401°S, 46.206°E; 14 Mar. 1985; P. Mundel & Philip leg.; engineer shed, station; USNM.

#### A1.10. *Spermophora* sp. “Mal2”

**Remarks.** This undescribed species is very similar to some species of *Spermophora* described from Southeast Asia (e.g., *S. kerinci* Huber, 2005; *S. tumbang* Huber, 2005; *S. dumoga* Huber, 2005), and possibly identical to “S282 *Spermophora* Mal2 Mal213” in Eberle et al. (2018) and Huber et al. (2018), originating from Singapore.

**New records.** SEYCHELLES – **Mahé** • 2 ♂♂, 5 ♀♀; Port Glaud, near Cap Ternay; 4.6452°S, 55.3883°E; 40 m a.s.l.; 4 Mar. 2013; C. Hoareau leg.; ZFMK Ar 23929 • 3 ♀♀, 1 juv., in pure ethanol; same data as preceding;

ZFMK Sey23 • 3 ♂♂, 5 ♀♀; Anse Boileau, Glacis La Reserve; 4.7070°S, 55.5007°E; 230 m a.s.l.; 7 Mar. 2013; C. Hoareau leg.; ZFMK Ar 23930 • 1 ♀, in pure ethanol; same data as preceding; ZFMK Sey26.

#### A1.11. *Spermophorides lascars* Saaristo, 2001

**Remarks.** Only known from the type series from Silhouette (Saaristo 2001). The generic assignment of this species is dubious (Huber 2007). It is also unclear whether this is a native or an introduced species.

#### A1.12. *Uthina luzonica* Simon, 1893

**Remarks.** Widely distributed, introduced to the Seychelles; origin East Asia. Numerous previous records from Mahé, Praslin, and Silhouette (Saaristo 2001; Yao et al. 2016).

**New records.** SEYCHELLES – **Mahé** • 3 ♀♀; Port Glaud, near Cap Ternay; 4.6452°S, 55.3883°E; 40 m a.s.l.; 4 Mar. 2013; C. Hoareau leg.; ZFMK Ar 23931 • 2 ♂♂, 1 ♀; Baie Lazare; 4.7562°S, 55.4732°E; 25 m a.s.l.; 5 Mar. 2013; C. Hoareau leg.; ZFMK Ar 23932 • 1 ♂; Bel Ombre; 4.6215°S, 55.3957°E; 70 m a.s.l.; 6 Mar. 2013; C. Hoareau leg.; ZFMK Ar 23933 • 1 ♀; Anse Boileau, Glacis La Reserve; 4.7070°S, 55.5007°E; 230 m a.s.l.; 7 Mar. 2013; C. Hoareau leg.; ZFMK Ar 23934.

## Supplementary material 1

### Figure S1

**Authors:** Huber BA, Meng G (2023)

**Data type:** .pdf

**Explanation note:** Best maximum-likelihood tree found by IQ-TREE with CO1 barcode, 12S, 16S, 18S, 28S and H3 of all specimens. The gene alignments were trimmed with the ClipKIT\_smart-gap strategy. Best-fit model determined by the ModelFinder in IQ-TREE: GTR+F+R7. The “+”/“–” symbols mean that other trees support/do not support the respective node. The other trees were constructed from the gene alignments being trimmed with ClipKIT\_gappy, ClipKIT\_kpi-gappy, ClipKIT\_kpi-smart-gap, ClipKIT\_kpi, ClipKIT\_kpic-gappy, ClipKIT\_kpic-smart-gap, ClipKIT\_kpic, Gblocks, TrimAl (-automated 1) strategies, respectively. Branch support values are ultrafast bootstrap (UFBoot) supports (%). Tip labels are composed of the specimen’s code, species name, and collection vial number.

**Copyright notice:** This dataset is made available under the Open Database License (<http://opendatacommons.org/licenses/odbl/1.0>). The Open Database License (ODbL) is a license agreement intended to allow users to freely share, modify, and use this Dataset while maintaining this same freedom for others, provided that the original source and author(s) are credited.

**Link:** <https://doi.org/10.3897/asp.81.e86793.suppl1>

## Supplementary material 2

### Figure S2

**Authors:** Huber BA, Meng G (2023)

**Data type:** .pdf

**Explanation note:** Best maximum-likelihood tree found by IQ-TREE with CO1 barcode, 12S, 16S, 18S, 28S and H3 of all specimens but rogue taxa excluded. The gene alignments were trimmed with the ClipKIT\_smart-gap strategy. Best-fit model determined by the ModelFinder in IQ-TREE: GTR+F+R7. The “+”/“–” symbols mean that other trees support/do not support the respective node. The other trees were constructed from the gene alignments being trimmed with ClipKIT\_gappy, ClipKIT\_kpi-gappy, ClipKIT\_kpi-smart-gap, ClipKIT\_kpi, ClipKIT\_kpic-gappy, ClipKIT\_kpic-smart-gap, ClipKIT\_kpic, Gblocks, TrimAl (-automated 1) strategies, respectively. Branch support values are ultrafast bootstrap (UFBoot) supports (%). Tip labels are composed of the specimen’s code, species name, and collection vial number.

**Copyright notice:** This dataset is made available under the Open Database License (<http://opendatacommons.org/licenses/odbl/1.0>). The Open Database License (ODbL) is a license agreement intended to allow users to freely share, modify, and use this Dataset while maintaining this same freedom for others, provided that the original source and author(s) are credited.

**Link:** <https://doi.org/10.3897/asp.81.e86793.suppl2>